THE JOURNAL OF PHYSICAL CHEMISTRY A

pubs.acs.org/JPCA

Feature Article

Nonadiabatic Molecular Dynamics at Metal Surfaces

Wenjie Dou* and Joseph E. Subotnik*

Cite This: https://dx.doi.org/10.1021/acs.jpca.9b10698

Read Online

ACCESS | Metrics & More | Article Recommendations

ABSTRACT: Dynamics at molecule−metal interfaces are a subject of intense current interest and come in many different flavors of experiments: gas-phase scattering, chemisorption, electrochemistry, nanojunction transport, and heterogeneous catalysis, to name a few. These dynamics involve nuclear degrees of freedom entangled with many electronic degrees of freedom (in the metal), and as such there is always the possibility for nonadiabatic phenomena to appear: the nuclei do not necessarily need to move slower than the electrons to break the Born−Oppenheimer (BO) approximation. In this Feature Article, we review a set of dynamical methods developed recently to deal with such nonadiabatic phenomena at a metal surface, methods that serve as alternatives to Tully's independent electron surface hopping (IESH) model. In the weak molecule−metal coupling regime, a classical master equation (CME) can be derived and a simple surface hopping approach is proposed to propagate nuclear and electronic dynamics stochastically. In the strong molecule−metal interaction regime, a Fokker−Planck equation can be derived for the nuclear dynamics, with electronic DoFs incorporated into the overall friction and random force. Lastly, a broadened classical master equation (BCME) can interpolate between the weak and strong molecule−metal interactions. Here, we briefly review these methods and the relevant benchmarking data, showing in particular how the methods can be used to calculate nonequilibrium transport properties. We highlight several open questions and pose several avenues for future study.

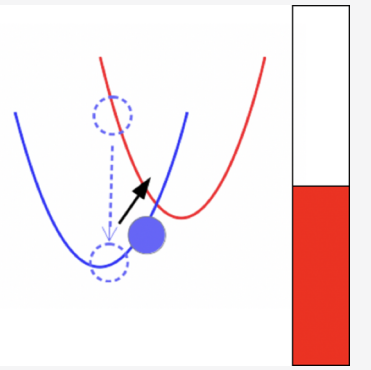

1. INTRODUCTION

The Born−Oppenheimer approximation plays a central role in modern physics and chemistry, asserting that nuclear motion is decoupled from electronic dynamics due to the large ratio of the mass of a nucleus to the mass of an electron. For many chemical processes, however, several excited electronic states are relevant, and the Born−Oppenheimer approximation breaks down, e.g., for processes with electronic relaxation or electron and energy transfer. And at molecule−metal interfaces, electrons from the metal are much easier to excite than for an isolated molecule, such that Born−Oppenheimer dynamics can break down even more dramatically. Such nonadiabatic dynamics at molecule−metal interfaces are relevant for many typical chemical setups, e.g., chemisorption,[1−4] electrochemistry,[5−8] heterogeneous catalysis,[9−11] and molecular junctions.[12,13]

Before addressing the role of the metal surface, consider for a moment a simple, nonadiabatic event for a photoexcited molecule in the gas phase or in solution, with only a handful of electronic states. For such an experiment, a variety of computational approaches have been developed to treat coupled electron−nuclear dynamics including: generalized master equations,[14,15] the Meyer−Miller mapping,[16−18] the momentum jump approximation,[19] linearized path integrals,[20] multiple spawning,[21] and exact factorization dynamics.[22] Among these approaches, Ehrenfest dynamics (ED) and Tully's fewest switch surface hopping (FSSH)[23] are probably still the most commonly used approaches, in no small part due to their simplicity. Nowadays, many researchers continue to look for improvements to these approaches, e.g., by addressing the coherence problem of FSSH[24,25] or the detailed balance problem of ED.[26] At the same time, it is also routine nowadays for computational physicists and chemists to use FSSH and ED to model a variety of photochemical processes, e.g., light-harvesting, proton coupled electron transfer,[6,27] singlet fission,[28] and multidimensional spectroscopy.[29−31]

Turning to the case of molecules on surfaces, we note that, near a metal surface, because of the continuum of electronic degrees of freedom (DoFs), nonadiabatic dynamics are much more complicated than they are in solution. For these problems, while numerically exact solutions for simple model Hamiltonians can sometimes be ascertained, e.g., through multiconfiguration time dependent Hartree (MCTDH),[32] quantum Monte Carlo (QMC),[33] or the hierarchical quantum master equation (HQME),[34,35] more commonly we require new insights based on a reasonable physical approximation, and these approximations lead us to simpler descriptions of the problem, e.g., such as a quantum master equation,[36−38] scattering matrix,[39,40] a Green's function approach,[41−44] or

Received: November 14, 2019
Revised: January 7, 2020
Published: January 9, 2020

influence functional techniques.[45] For the purposes of modeling realistic systems, however, even these approaches are usually still too difficult, and new, affordable, and accurate approaches are still being actively developed. And thus, we return to the most basic dynamical propagation routines: Ehrenfest dynamics and surface hopping dynamics.

(i) From a mean-field, Ehrenfest point of view, the dynamics of molecules near a metal surface is one whereby, just as for standard Born−Oppenheimer dynamics, nuclei evolve on a potential of mean force. If one goes beyond the Born−Oppenheimer approximation and works at first order in the nonadiabaticity of the molecular dynamics, the influence of the collective electronic DoFs gives rise to frictional (damping) and fluctuating (random) forces.[46,47] Such an "electronic friction" model has been explored by many researchers in the literature over decades.[4,40,48−52] In particular, the most commonly used expression was extrapolated by Head-Gordon and Tully (HGT),[53] which has been implemented to study several realistic systems, including vibrational relaxation and chemisorption.[10,11,54−64] As detailed below, we have recently shown that Langevin dynamics can be rigorously derived from a quantum-classical Liouville equation (QCLE)[46] and the resulting HGT model agrees with several other electronic friction models.[65,66] Furthermore, we have demonstrated that nonadiabatic effects can give rise to quantifiable entropy production.[67]

Of course, there are cases where electronic friction fails to recover exact dynamics at metal surfaces.[47,68,69] After all, the electronic friction serves as a first-order correction to the BO approximation.[46,53] When strong nonadiabatic dynamics occur, i.e., nuclear DoFs are not slow compared to electronic DoFs, a mean-field treatment of coupled electron−nuclear dynamics is not valid. Moreover, because the frictional approach traces out all electronic dynamics, a detailed understanding of the electron transfer, spin dynamics, etc. is missing in the electronic friction picture. To go beyond this mean-field solution, a surface hopping picture serves as a better alternative.

(ii) From a surface hopping point of view, the usual algorithm for simulating dynamics at surfaces is the independent electron surface hopping (IESH) approach as developed by Shenvi, Roy, and Tully.[70,71] According to IESH, one explicitly discretizes the continuum of electronic DoFs and then uses FSSH to evolve the mixed quantum-classical dynamics. To make the computational cost affordable while still treating many electronic states, the Hamiltonian models independent electrons such that the electronic wave function is always the simple product of one-electron orbitals. In practice, the IESH algorithm is a powerful approach for simulating dynamics at surfaces,[70,71] and we have recently demonstrated that IESH does agree with Marcus theory under the right conditions.[72] The only hiccup with IESH is that, for gas-phase scattering calculations (i.e., without a nuclear bath), there is no natural means to include electronic relaxation of the Fermi sea bath to the Fermi level without introducing artifacts;[72] this remains an outstanding question for future development.

Now within the context of surface hopping calculations, we have recently developed a few alternative approaches that do automatically reach the correct equilibrium conditions. (a) First, instead of treating all metallic electrons explicitly, the methods assume that one can separate molecular electrons (at least partially) from the electronic DoFs in the metal.[38,73] Thereafter, in the limit of weak molecule−metal interactions, we arrive at a simple classical master equation (CME). This CME has a simple surface hopping interpretation: we run trajectories on potential energy surfaces (PESs) of the molecular system, and we introduce hopping between potential energy surfaces to account for molecule−metal interactions. To be specific, the hopping probabilities depend on (i) the hybridization function of the molecule−metal couplings and (ii) the energy of the impurity orbital relative to the Fermi level of the metallic electrons. As shown below, one of the most important features of the CME is that one can directly relate CME dynamics to mean-field electronic friction dynamics: when electronic dynamics are faster than nuclear motion, CME surface hopping can be mapped onto classical motion on potential of mean force plus electronic friction and random force. See Figure 1 and ref 74. (b)

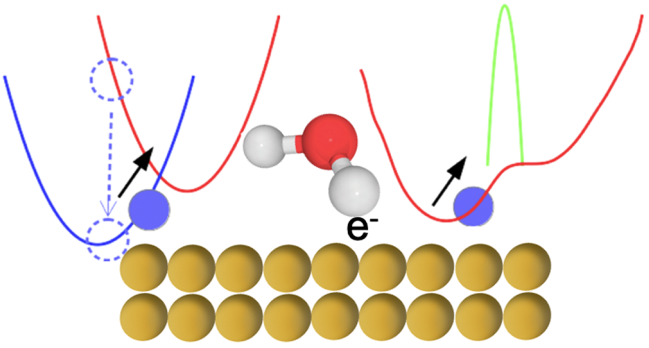

Figure 1. Surface hopping and electronic friction molecular dynamics at metal surfaces. In the surface hopping picture, electron transfer between the molecule and metal surface is incorporated into hopping events between neutral and changed potential energy surfaces. In the electronic friction picture, we propagate molecular dynamics along the potential of mean force, while the electronic dynamics are incorporated into a frictional force and a fluctuating force. There are natural connections between the surface hopping and electronic friction pictures. As shown in section 3.2, when the hopping between the neutral and charged states occurs quickly, i.e., electrons move very fast, surface hopping dynamics recover molecular dynamics on a potential of mean force, with the hopping being reduced into both a frictional and a random force.

Second, armed with this surface-hopping/friction connection, we have demonstrated that one reasonable means to incorporate broadening effects into surface hopping dynamics is simply to adjust the diabatic surfaces of propagation so as to recover the correct, broadened potential of mean force.[75] As shown below, such a "broadened" classical master equation (BCME) appears to be very accurate for treating both weak and strong molecule−metal interactions (as benchmarked against numerical exact results).[76]

The present Feature Article is not intended by any means to be an exhaustive review of dynamics near metal surfaces; for such a purpose, see refs 69 and 77−82. Instead, our purpose here is to highlight our own perspective in this field and what we have learned over the past few years of our investigations. We organize this article as follows. In section 2, we introduce the Anderson−Holstein model (which will serve as the model Hamiltonian of choice) and we give a brief overview of methods for solving the AH problem. In section 3.1, we introduce the classical master equation (CME). In section 3.2 we demonstrate a useful connection between the CME and an electronic friction model. Armed with this connection, in section 3.3, we introduce the BCME, which we have found to be a very efficient and accurate approach as far as simulating the dynamics of a single molecule on a surface. Next, in section 4, we show key numerical

https://dx.doi.org/10.1021/acs.jpca.9b10698
J. Phys. Chem. A XXXX, XXX, XXX−XXX

results from these dynamical methods. In section 5, we show how to embed the CME into a QCLE to model nonadiabatic dynamics for a molecule (with many orbitals) and a metal surface. In section 6, we pose several open questions and point out future directions for newcomers to the field.

2. THE ANDERSON–HOLSTEIN MODEL

To describe nonadiabatic molecular dynamics near metal surfaces, we begin with the standard model of choice: the Anderson–Holstein (AH) model (or the Anderson–Newns model in the surface scicence community).[83−85] The AH model posits a molecule with only a single electronic level coupled to both a manifold of electrons and a set of nuclear degrees of freedom (DoFs). To be explicit, in the AH model, the total Hamiltonian is divided into three parts: the system $\hat{H}_s$, the bath $\hat{H}_b$, and the interactions between the system and bath $\hat{H}_I$,

$$\hat{H} = \hat{H}_s + \hat{H}_b + \hat{H}_I \tag{1}$$

$$\hat{H}_s = h(\mathbf{R})\hat{d}^+\hat{d} + U_0(\mathbf{R}) + \sum_\alpha \frac{P_\alpha^2}{2m_\alpha} \tag{2}$$

$$\hat{H}_b = \sum_k \epsilon_k \hat{c}_k^+ \hat{c}_k \tag{3}$$

$$\hat{H}_I = \sum_k V_k(\mathbf{R})(\hat{d}^+\hat{c}_k + \hat{c}_k^+\hat{d}) \tag{4}$$

Here $\hat{d}$ ($\hat{d}^+$) is the annihilation (creation) operator for the electronic orbital of the molecule. $\hat{c}_k$ ($\hat{c}_k^+$) is the annihilation (creation) operator for the kth electronic orbital in the metal. $\mathbf{R}$ and $\mathbf{P}$ are nuclear positions and momenta, respectively (we use α and ν to denote the nuclear degrees of freedom). $U_0(\mathbf{R})$ is the nuclear potential for the neutral molecule, i.e., $\hat{d}^+\hat{d} = 0$; when the molecule is charged, i.e., $\hat{d}^+\hat{d} = 1$, the nuclear potential is $U_1(\mathbf{R}) = U_0(\mathbf{R}) + h(\mathbf{R})$. $V_k(\mathbf{R})$ is the coupling between the molecular orbital d and the metallic orbital k, which generally depends on $\mathbf{R}$. We will define a hybridization function Γ to characterize the strength of the system-bath coupling:

$$\Gamma(\epsilon) = 2\pi \sum_k V_k^2 \delta(\epsilon - \epsilon_k) \tag{5}$$

Γ typically depends on ϵ (through the δ function in the above equation) and nuclear position $\mathbf{R}$ (through V_k). To simplify the model, typically the wide-band limit is applied, such that Γ is independent of ϵ.

As far as the molecule is concerned, the AH model represents an open quantum system, and one would like to use the Fermi energy μ and the temperature kT of the electronic bath to propagate molecular dynamics. For the nonequilibrium case, e.g., molecular junctions, where there are two metals with two different Fermi levels and there can be an electronic current flowing through the molecule, one must use kT, μ_L, and μ_R to propagate dynamics. In the following, we will mostly focus on the equilibrium case; for extensions to the nonequilibrium case, see section 4.2.

2.1. Regimes of the AH Model. In practice, propagating AH dynamics rigorously is difficult due to (1) the presence of a manifold of electronic DoFs in the metal (so that the computational cost grows exponentially with the increasing number of quantum electrons) and (2) the nonadiabaticity of the dynamics (whereby electronic dynamics and nuclear motion are coupled). To be more explicit with regard to the question of nonadiabaticity, consider the hybridization function Γ, which is often used to quantify the decay of the d electron on the molecule: the typical time scale for electronic motion is characterized by $\hbar/\Gamma$. At the same time, consider also the nuclear potential U_0, according to which one can extract the frequency ω_α for a certain nuclear mode, where $\omega_\alpha = \sqrt{\partial_\alpha^2 U_0/m_\alpha}$: the typical time scale for nuclear motion can be quantified as $1/\omega_\alpha$. The ratio of the two time scales can then used to classify the AH model into two regimes:

- the nonadiabatic regime, $\Gamma < \hbar\omega_\alpha$, i.e., where nuclear motion is fast compared to electronic dynamics
- the adiabatic regime, $\Gamma > \hbar\omega_\alpha$, i.e., where nuclear motion is slow compared to electronic dynamics

In addition to the two energy scales above, there is also a third energy scale that plays a role in the dynamics that should be taken into account: temperature, kT. Depending on the strength of the molecule–metal coupling compared to temperature, we can further classify the AH model:

- the weak molecule–metal interaction regime, $kT > \Gamma$
- the strong molecule–metal interaction regime, $kT < \Gamma$

Lastly, yet another classification can be made as well: is the AH model in the regime of classical nuclear motion ($kT > \hbar\omega_\alpha$) or the regime of quantum mechanical nuclear motion ($kT < \hbar\omega_\alpha$)?

Note that all of the classifications above can be overlapped and are not necessarily unique. For example, for classical nuclei ($kT > \hbar\omega_\alpha$), the strong molecule–metal interactions regime ($\Gamma > kT$) automatically lies in the adiabatic regime ($\Gamma > \hbar\omega_\alpha$); similarly, the nonadiabatic regime ($\Gamma < \hbar\omega_\alpha$) automatically lies in the weak molecule–metal interaction regime ($\Gamma < kT$). The fact that these regimes overlap well will allow us (below) to rationalize the BCME approach as an extrapolation from the weak to strong molecule–metal interaction regimes as well as from the nonadiabatic to adiabatic regimes.

2.2. Flowchart of the Different Methods for Different Regimes. As stated previously, because computational cost scales exponentially with the number of quantum DoFs, a full quantum mechanical treatment of the AH model (with no approximations) can be very expensive. So far, only a few computational approaches are available and only for relatively small systems, e.g., MCTDH,[32] QMC,[33] and the HQME[34,35] approaches. When one wishes to model a more realistic system, assumptions and approximations must be made. To that end, the classification of the different AH regimes in the previous subsection is a good guide for understanding the existing semiclassical literature. For visual ease, our discussion below will follow Figure 2, which should help the reader understand the panoply of different mixed quantum classical approaches possible.

In the limit where the temperature is high relative to the typical frequency of the nuclear modes $kT > \hbar\omega_\alpha$, we can simplify AH dynamics by treating the low frequency nuclear modes classically. If one makes no further assumptions and discretizes the electronic bath explicitly, one standard approach today is the independent electronic surface hopping (IESH) model of Shenvi, Roy, and Tully.[70] As discussed above, IESH is a generalization of the FSSH model, whereby one propagates dynamics over a very large number of electronic states, with individual electrons allowed to hop independently. This scheme accounts for electron–hole pair excitation and can recover some energy relaxation for a scattering event.[70,71] That being said, the computational cost of IESH is not always small and the scheme

https://dx.doi.org/10.1021/acs.jpca.9b10698
J. Phys. Chem. A XXXX, XXX, XXX−XXX

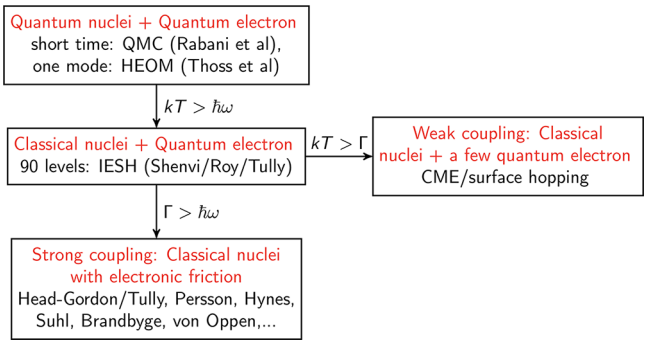

Figure 2. Regimes of the AH model. In the limit $kT > \hbar\omega$, we can treat nuclear motion classically. To further simplify the dynamics, two additional approximations are taken. (1) In the weak molecule−metal interaction regime $kT > \Gamma$, we treat out electronic degrees of freedom in the metal, and we arrive at a CME. (2) In the adiabatic regime, $\Gamma > \hbar\omega$, where electron is faster than nuclei, we trace out all electronic degrees of freedom, and we arrive at Langevin dynamics for the classical nuclei.

can have problems achieving the correct detailed balance at equilibrium. IESH will be discussed in section 4.3.

Next, if we insist on finding the correct equilibrium density matrix according to a proper (but limited) description of electronic dissipation, according to Figure 2 and as discussed in the Introduction, we have two options. First, in the limit of weak molecule−metal interaction, i.e., $kT > \Gamma$, we can trace out the electronic DoFs in the metal, which leads to a very inexpensive classical master equation (CME). Similar to Tully's FSSH algorithm, the CME propagates nuclear motion with hops between electronic levels, but unlike Tully's FSSH algorithm, energy is not conserved, so that no momentum adjustment is taken when electron transitions occur. This prescription yields a proper account of dissipation in the electronic bath such that detailed balance is obeyed. See section 3.1 for a detailed discussion.

Second, in the limit of strong molecule−metal interactions, i.e., $\Gamma > \hbar\omega_\alpha$, where the electrons are much faster than the nuclear motion, nuclear motion becomes adiabatic and another approach is optimal. Here, we can trace out *all* of the electronic DoFs and focus purely on the nuclear motion. To first order, the influence of the electronic dynamics can be written as a frictional force as well as a fluctuating force that corrects the Born−Oppenheimer approximation. At equilibrium, because the second fluctuation−dissipation theorem is obeyed by the so-called electronic friction tensor and corresponding random force, nuclear DoFs always reach thermal equilibrium. There is a long history of work on electronic friction in both the chemistry and physics literature.[4,40,48−53,86] See section 3.2 and refs 46, 47, 65, and 66 for details.

Below we will almost always assume that we are operating in the $kT > \hbar\omega_\alpha$ regime, such that a classical treatment of nuclear motion is feasible, and we will review the relevant quasi-classical methods from Figure 2 in more detail.

3. SEMICLASSICAL METHODS UNDER INVESTIGATION

3.1. Classical Master Equation/Surface Hopping (CME/SH). In the limit of relatively weak molecule−metal coupling (as compared with temperature, $\Gamma < kT$), one can treat the molecule−metal interaction perturbatively up to second order and, provided the nuclei are classical, one can derive a classical master equation for the coupled electron−nuclear dynamics of the molecule described by the AH model:

$$\frac{\partial}{\partial t}\rho_0(\mathbf{R},\mathbf{P},t) = -\sum_\alpha \frac{P_\alpha}{m_\alpha}\frac{\partial \rho_0}{\partial R_\alpha} + \sum_\alpha \frac{\partial U_0}{\partial R_\alpha}\frac{\partial \rho_0}{\partial P_\alpha} - \frac{\Gamma}{\hbar}f(h)\rho_0 + \frac{\Gamma}{\hbar}(1-f(h))\rho_1 \tag{6}$$

$$\frac{\partial}{\partial t}\rho_1(\mathbf{R},\mathbf{P},t) = -\sum_\alpha \frac{P_\alpha}{m_\alpha}\frac{\partial \rho_1}{\partial R_\alpha} + \sum_\alpha \frac{\partial U_1}{\partial R_\alpha}\frac{\partial \rho_1}{\partial P_\alpha} + \frac{\Gamma}{\hbar}f(h)\rho_0 - \frac{\Gamma}{\hbar}(1-f(h))\rho_1 \tag{7}$$

Here $\rho_0(\mathbf{R},\mathbf{P})$ and $\rho_1(\mathbf{R},\mathbf{P})$ are the probability densities in phase space for the neutral $(\hat{d}^+\hat{d}=0)$ and charged $(\hat{d}^+\hat{d}=1)$ molecule. These densities follow classical motion on potential energy surfaces $U_0(\mathbf{R})$ and $U_1(\mathbf{R})$ correspondingly, plus exchange between the two densities. Note that $U_1 = U_0 + h$, where $h(\mathbf{R})$ is the onsite energy of the d orbital (see eq 2); henceforward, we will often drop the dependence of h on $\mathbf{R}$ for notational convenience only. The exchange rate from ρ_0 to ρ_1 is $\frac{\Gamma}{\hbar}f(h)$, and the exchange rate from ρ_1 to ρ_0 is $\frac{\Gamma}{\hbar}(1-f(h))$. Here, $f(h) \equiv 1/(\exp((h-\mu)/kT)+1)$ is the Fermi function; note that $f(-h) = 1-f(h)$.

The CME has a simple surface hopping interpretation: if one uses a swarm of trajectories to represent the density probability, each trajectory follows classical motion on one of the two PESs:

$$\dot{R}_\alpha = \frac{P_\alpha}{m_\alpha} \tag{8}$$

$$\dot{P}_\alpha = -\frac{\partial U_\lambda}{\partial R_\alpha} \tag{9}$$

Here $\lambda = 0,1$ is the activate potential surface which represents current electronic states. The rate of switching from U_0 to U_1 is $\frac{\Gamma}{\hbar}f(h)$, and the rate of switching from U_1 to U_0 is $\frac{\Gamma}{\hbar}(1-f(h))$.

In Figure 3, we prepare different initial kinetic energies for a single nuclear mode and plot the average kinetic energy as a function of time according to eqs 6 and 7. We note that, at long times, the kinetic energy converges to the correct equilibrium solution, where the average kinetic energy is one-half kT, $E_k = \frac{1}{2}kT$. In ref 73, we further show that the final position and momentum distributions have the correct Gaussian shapes with widths kT. Note that CME dynamics are consistent with the surface scattering experiments by Wodtke and co-workers,[2] where one observes huge vibrational energy loss of NO molecule after scattering back from a gold metal surface. From the surface hopping perspective, Wodtke et al. have argued that this energy loss arises from hopping back and forth between the NO and NO^- potentials. Of course, in the case of an insulator, no such transition is allowed and there is no such dissipation of energy. Interestingly, Figure 3 also shows there will be energy promotion if one starts from a low initial kinetic energy, and such energy promotion has been observed in scattering events by Wodtke and co-workers.[87]

3.1.1. CME Surface Hopping vs Tully's FSSH. For the interested reader, it is worthwhile to emphasize a few key differences between CME surface hopping (dealing with nonadiabatic dynamics near metal surfaces) and Tully's fewest

https://dx.doi.org/10.1021/acs.jpca.9b10698
J. Phys. Chem. A XXXX, XXX, XXX−XXX

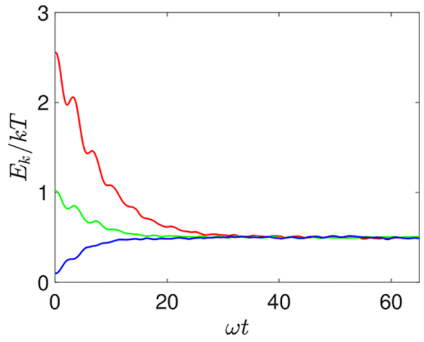

Figure 3. Average vibrational energy as a function of time from a CME surface hopping solution. We note that, regardless of different initial conditions, we arrive at one equilibrium solution, where $E_k = \frac{1}{2}kT$. In ref 73, we further show the momentum distribution obeys Gaussian distribution with width equal to kT, meaning the nuclear DoFs reach thermal equilibrium with the electrons in the metal. We are considering here a single nuclear mode where $U_0 = \frac{1}{2}m\omega^2x^2$ and $h = \epsilon_d + gx\sqrt{2m\omega/\hbar}$, with $\hbar\omega = 0.003$, $kT = 0.01$, $g = 0.0075$, $\Gamma = 0.005$ (all in atomic units).

switch surface hopping (FSSH) (dealing with nonadiabatic dynamics in gas phase or solution).

1. For CME surface hopping, hops are governed by an effective coupling Γ and Fermi function $f(h)$, which together guarantee that detailed balance is satisfied *exactly*. By contrast, for Tully's FSSH, hops are governed by a combination of an electronic amplitude, the local derivative coupling, and the concept of velocity rescaling. For this reason, detailed balance is obtained only *approximately* for FSSH.[88]
2. Unlike Tully's FSSH, there is no rescaling velocities ever within the CME and energy is not conserved for CME dynamics: the molecular system is explicitly open because of the metal bath.
3. For Tully's FSSH, because one propagates electronic amplitudes forward in time no matter how the nuclear motion may be different for different adiabatic states, it is well-known that FSSH can suffer from overcoherence.[23−25,89−91] By contrast, for CME surface hopping, the hopping rate is determined purely by the local position; no electronic density is needed or propagated, and there are never any coherence issues. In short, the question of coherence between two molecular states with different numbers of electrons is not terribly important. That being said, as shown in section 5, when dealing with a large molecule and many quantum levels (some with the same number of electrons), coherence/decoherence issues can and do arise.[92]

3.1.2. CME and Broadening. Before we conclude this section, one final word is now appropriate regarding the CME. Even though the CME works well in the weak molecule−metal interaction regime, the CME is missing all so-called broadening effects. To understand these effects, we note that the CME has a simple steady solution: $\rho_0 = C\exp(-U_0/kT)$ and $\rho_1 = C\exp(-U_1/kT)$, where C is a normalization factor that satisfies $\int\sum_\alpha dR_\alpha\, dP_\alpha\,(\rho_0 + \rho_1) = 1$. Henceforward, electronic populations are evaluated by averaging over all nuclear distributions, e.g., $P_1 = \int\sum_\alpha dR_\alpha\, dP_\alpha\,\rho_1$ yields the total probability for the molecule to be charged. For the AH model in eqs 1−4 with linearly dependence of h on one nuclear coordinate x ($h = \epsilon_d + gx\sqrt{2m\omega/\hbar}$) plus parabolic potential for the nuclei $\left(U_0(x) = \frac{1}{2}m\omega^2x^2\right)$, one finds that the steady state solution in phase space is

$$\rho_0^{eq}(x,p) = \frac{\beta\omega}{2\pi}\frac{1}{1+e^{-\beta(\epsilon_d - g^2/\hbar\omega)}}e^{-\beta((1/2)m\omega^2x^2+(p^2/2m))}$$

and

$$\rho_1^{eq}(x,p) = e^{-\beta(\epsilon_d+gx\sqrt{2m\omega/\hbar})}\rho_0^{eq}(x,p)$$

Thus, the procedure above concludes that the total population of the molecule is a single Fermi distribution with renormalized energy level $\bar{\epsilon}_d$, $P_1 = f(\bar{\epsilon}_d)$, where $\bar{\epsilon}_d = \epsilon_d - E_r$; here $E_r = g^2/\hbar\omega$ is the reorganization energy.[38,73] Unfortunately, this answer is incorrect. The correct answer is not a Fermi function in general, but rather the integral of a convolution of a Fermi function with a Lorentzian:[93]

$$n(h(x)) = \int\frac{d\epsilon}{2\pi}\frac{\Gamma}{(\epsilon - h(x))^2 + (\Gamma/2)^2}f(\epsilon) \tag{10}$$

$$P_1 = \frac{1}{Z}\int n(h(x))e^{-\beta U_{pmf}(x)}\,dx \tag{11}$$

Here, U_{pmf} is the potential of mean force,

$$U_{pmf}(x) = U_0(x) + \int_{x_0}^{x}\frac{\partial h(x')}{\partial x'}n(h(x'))\,dx' \tag{12}$$

and Z is a normalization factor, $Z = \int e^{-\beta U_{pmf}(x)}dx$. Henceforward, we will refer to eq 11 as a broadened population, and anywhere a lorentzian of width Γ appears, will refer to the notion of "broadening." See sections 3.2 and 3.3 and ref 93. In practice, the CME is correct only in the limit that $\Gamma \to 0$. See also section 3.3 for a discussion of broadening and how to incorporate broadening effects within the CME.

3.2. Fokker−Planck (FP) Equation/Electronic Friction. *3.2.1. Friction in Full Generality (with Broadening).* At this point, let us turn to the adiabatic limit, where electronic dynamics are faster than nuclear dynamics. In such a limit, one can trace out all of the electronic DoFs, leaving purely classical nuclear DoFs with additional frictional and fluctuating forces to capture the electronic response:

$$m_\alpha\ddot{R}_\alpha = \bar{F}_\alpha - \sum_\nu \gamma_{\alpha\nu}\dot{R}_\nu + \delta F_\alpha \tag{13}$$

Here $\bar{F}_\alpha$ is the mean force, $\gamma_{\alpha\beta}$ is the "electronic friction" coefficient (which operates on the nuclei), and δF_α is the random force. According to eq 13, perhaps surprisingly, whenever a molecule operates near a metal surface, there will *always* be some friction and random forces associated with the construction and destruction of electron hole pairs.

In order to derive the Markovian Langevin dynamics in eq 13 (with explicit expressions for the mean force $\bar{F}_\alpha$, friction $\gamma_{\alpha\nu}$, and random force δF_α), the most general procedure is to invoke the mixed quantum-classical Liouville equation (QCLE),[19,94,95] and impose an adiabatic expansion in the velocity of the nuclear motion.[46] In such a way, one can extract the proper electronic friction tensor that is valid in or out of equilibrium. See ref 46 and the supporting information within for such a derivation. The results for $\bar{F}_\alpha$ and $\gamma_{\alpha\nu}$ within the AH model are as follows:

https://dx.doi.org/10.1021/acs.jpca.9b10698
J. Phys. Chem. A XXXX, XXX, XXX−XXX

$$\bar{F}_\alpha = -\frac{\partial U_0}{\partial R_\alpha} - \frac{\partial h}{\partial R_\alpha} n(h) \tag{14}$$

$$\gamma_{\alpha\nu} = -\frac{\hbar}{2}\frac{\partial h}{\partial R_\alpha}\frac{\partial h}{\partial R_\nu}\int \frac{d\epsilon}{2\pi}\left(\frac{\Gamma}{(\epsilon - h)^2 + (\Gamma/2)^2}\right)^2 \frac{\partial f(\epsilon)}{\partial \epsilon} \tag{15}$$

Here, $n(h)$ in eq 14 is the local equilibrium electronic population with broadening taken into account (see eq 10). Due to the strong interaction between molecule and metal, the molecular d level is not a single discrete level. Instead, the discrete level has been broadened by a Lorentzian with half-width Γ. The local equilibrium electronic population ($n(h)$) is then a convolution of the Fermi distribution with a Lorentzian, and the total electronic population is the integral of $n(h)$ over all space, weighted by $e^{-\beta U_{pmf}}$. See eqs 10−12. Henceforward, we will refer to FP dynamics with the correctly broadened force (eq 14) and the correctly broadened friction (eq 15) as a broadened FP (BFP) equation. In the limit where $\Gamma < kT$, broadening is small compared to the width of the Fermi distribution, such that $n(h) \to f(h)$, and the true mean force ($\bar{F}_\alpha$ in eq 14) recovers the unbroadened mean force from the CME ($\bar{F}_\alpha^{CME}$ in eq 22, see below).

Besides invoking the QCLE, various other techniques have also been proposed for calculating electronic friction tensors,[4,40,48−53,86] with some non-Markovian friction tensors also considered.[45,47,48,51,96] Although Langevin dynamics need not have any immediate connection to the QCLE, they arise naturally whenever one invokes an adiabatic approximation for one DoF that is coupled to a set of much faster DoFs; in that situation, as is well-known from chemical dynamics,[97] the general form of a friction tensor can be recast as a response function.[46,47]

3.2.2. Friction without Broadening. While the QCLE is the most general means to derive an electronic friction tensor, given the generality of Langevin dynamics, one must presume there should also be a means to map the simple CME above (in eq 6 and 7) onto Langevin dynamics as well. In order to establish such a mapping, notice that, without nuclear motion, the hopping in the CME (see eqs 6 and 7) gives a local equilibrium solution, $\rho_0 = A(1 - f(h))$ and $\rho_1 = Af(h)$, where A is the total probability density for the nuclear DoFs: $A = \rho_0 + \rho_1$. With nuclear motion, we can define a probability density B that quantifies the difference between ρ_0 and ρ_1 and the local equilibrium solution, i.e.

$$\rho_0(\mathbf{R},\mathbf{P}) = A(\mathbf{R},\mathbf{P})(1 - f(h)) + B(\mathbf{R},\mathbf{P}) \tag{16}$$

$$\rho_1(\mathbf{R},\mathbf{P}) = A(\mathbf{R},\mathbf{P})f(h) - B(\mathbf{R},\mathbf{P}) \tag{17}$$

Henceforward, we will call B the nonadiabatic probability density, since B quantifies how far away the local probability density is from local equilibrium due to nuclear motion.

If we plug the definitions in eqs 16 and 17 into the equations of motion in eqs 6 and 7, we arrive at

$$\frac{\partial A}{\partial t} = -\sum_\alpha \frac{P_\alpha}{m_\alpha}\frac{\partial A}{\partial P_\alpha} + \sum_\alpha \left(\frac{\partial U_0}{\partial R_\alpha} + \frac{\partial h}{\partial R_\alpha} f(h)\right)\frac{\partial A}{\partial P_\alpha} + \sum_\alpha \frac{\partial h}{\partial R_\alpha}\frac{\partial B}{\partial P_\alpha} \tag{18}$$

$$\frac{\partial B}{\partial t} = -\sum_\alpha \frac{P_\alpha}{m_\alpha}\frac{\partial B}{\partial R_\alpha} + \sum_\alpha \left(\frac{\partial U_0}{\partial R_\alpha} + \frac{\partial h}{\partial R_\alpha}(1 - f(h))\right)\frac{\partial B}{\partial P_\alpha} + \sum_\alpha \frac{\partial h}{\partial R_\alpha} f(h)(1 - f(h))\frac{\partial A}{\partial P_\alpha} + \sum_\alpha \frac{P_\alpha}{m_\alpha} A \frac{\partial f(h)}{\partial R_\alpha} - \frac{\Gamma}{\hbar} B \tag{19}$$

The first two terms on the right-hand side (RHS) of eq 18 indicate that A follows classical motion subjected to a mean force $\bar{F}_\alpha^{CME} = -\frac{\partial U_0}{\partial R_\alpha} - \frac{\partial h}{\partial R_\alpha} f(h)$. Similarly, the first two terms on the RHS of eq 19 indicate that B follows classical motion subject to a force $-\frac{\partial U_0}{\partial R_\alpha} - \frac{\partial h}{\partial R_\alpha}(1 - f(h))$. The last term on the RHS of eq 19 indicates that B decays at a rate $\Gamma/\hbar$. Obviously, A and B are coupled through the rest of the terms in eqs 18 and 19.

Finally, at this point we can impose our adiabatic approximation: since the electrons are presumed to be faster than the nuclei, the nonadiabatic density B should be small compared to the total probability density A; in addition, the decay in the last term on the RHS of eq 19 should dominate the classical motion expressed by the first two terms on the RHS of eq 19. Thus, we can approximate eq 19 as follows:

$$0 = \sum_\alpha \frac{\partial h}{\partial R_\alpha} f(h)(1 - f(h))\frac{\partial A}{\partial P_\alpha} + \sum_\alpha \frac{P_\alpha}{m_\alpha} A \frac{\partial f(h)}{\partial R_\alpha} - \frac{\Gamma}{\hbar} B \tag{20}$$

If we plug the solution for B to the above equation into eq 18, we arrive at an (unbroadened) Fokker−Planck (FP) equation,

$$\frac{\partial A}{\partial t} = -\sum_\alpha \frac{P_\alpha}{m_\alpha}\frac{\partial A}{\partial P_\alpha} - \sum_\alpha \bar{F}_\alpha^{CME}\frac{\partial A}{\partial P_\alpha} + \sum_{\alpha\nu} \gamma_{\alpha\nu}^{CME}\frac{\partial}{\partial P_\nu}\left(\frac{P_\alpha}{m_\alpha} A\right) + \sum_{\alpha\nu} D_{\alpha\nu}^{CME}\frac{\partial^2 A}{\partial R_\alpha \partial R_\nu} \tag{21}$$

Here the mean force $\bar{F}_\alpha^{CME}$, friction tensor $\gamma_{\alpha\nu}^{CME}$, and correlation function of the random force are expressed as

$$\bar{F}_\alpha^{CME} = -\frac{\partial U_0}{\partial R_\alpha} - \frac{\partial h}{\partial R_\alpha} f(h) \tag{22}$$

$$\gamma_{\alpha\nu}^{CME} = -\frac{\hbar}{\Gamma}\frac{\partial f(h)}{\partial R_\nu}\frac{\partial h}{\partial R_\alpha} \tag{23}$$

$$D_{\alpha\nu}^{CME} = \frac{\hbar}{\Gamma} f(h)(1 - f(h)\frac{\partial h}{\partial R_\alpha}\frac{\partial h}{\partial R_\nu} \tag{24}$$

The FP equation in eq 21 is equivalent to the Langevin equation in eq 13, with the random force satisfying the following statistics:

$$\langle \delta F_\alpha \rangle = 0 \tag{25}$$

$$\langle \delta F_\alpha(t)\, \delta F_\nu(t') \rangle = D_{\alpha\nu}^{CME}\delta(t - t') \tag{26}$$

Note also that eq 15 reduces to eq 23 (and eq 14 reduces to eq 22) in the limit that $\Gamma \to 0$, i.e., without any broadening. Finally, according to the properties of the Fermi function, $\frac{\partial f(h)}{\partial R_\nu} = -f(h)(1 - f(h))\frac{\partial h}{\partial R_\nu}/kT$ (kT is the temperature of the electrons), and the second fluctuation−dissipation theorem is demonstrably satisfied

$$D_{\alpha\nu}^{CME} = kT\gamma_{\alpha\nu}^{CME} \tag{27}$$

such that the classical modes in the Langevin equation or FP equation will reach thermal equilibrium with the same

https://dx.doi.org/10.1021/acs.jpca.9b10698
J. Phys. Chem. A XXXX, XXX, XXX−XXX

temperature as the electrons in the metal. Interestingly, the second fluctuation−dissipation theorem is hidden within the CME and can be revealed by mapping the CME onto a FP equation.

In Figure 4, we compare the nuclear dynamics from SH/CME and electronic friction-Langevin dynamics (EF-LD). We fix $\hbar\omega$ = 0.003, kT = 0.05 (in atomic units), and we vary Γ. In the case of larger Γ, SH agrees with EF-LD very well; by contrast, for the case of small Γ, EF-LD disagrees with SH, where EF-LD predicts that nuclear relaxation is too fast. Quite dramatically, the friction expression in eq 23 can be seen to diverge for infinitesimal Γ, indicating that EF-LD fails for small Γ. This curiosity will be discussed briefly later in section 3.3; see also ref 98 for more discussion of this point.

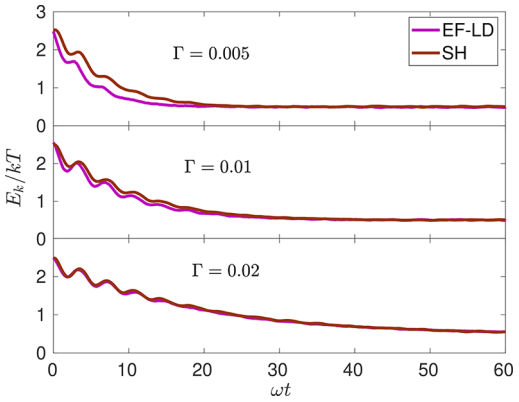

Figure 4. Average kinetic energy as a function of time from SH and EF-LD. Here we fix kT and $\hbar\omega$ and vary Γ. For larger Γ, SH agrees with EF-LD; by contrast, in the case of small Γ, EF-LD do not agree with SH. Note that SH must be correct for small Γ, indicating that EF-LD breaks down in such a limit. $\hbar\omega$ = 0.003, kT = 0.05 (all in atomic unit).[74]

3.3. Broadened Classical Master Equation (BCME).

Incorporating broadening into the CME framework can be done simply by modifying the diabatic potentials underlying eqs 6 and 7; we simply add the difference between the true mean force (eq 14) and the unbroadened mean force (eq 22). Hence one can propose new potentials $\tilde{U}_0$ and $\tilde{U}_1$ of the form

$$\frac{\partial \tilde{U}_0}{\partial R_\alpha} = \frac{\partial U_0}{\partial R_\alpha} - \bar{F}_\alpha + \bar{F}_\alpha^{\mathrm{CME}} \tag{28}$$

$$\frac{\partial \tilde{U}_1}{\partial R_\alpha} = \frac{\partial U_1}{\partial R_\alpha} - \bar{F}_\alpha + \bar{F}_\alpha^{\mathrm{CME}} \tag{29}$$

leading to a new CME of the form

$$\frac{\partial \rho_0}{\partial t} = -\sum_\alpha \frac{P_\alpha}{m_\alpha}\frac{\partial \rho_0}{\partial R_\alpha} + \sum_\alpha \frac{\partial \tilde{U}_0}{\partial R_\alpha}\frac{\partial \rho_0}{\partial P_\alpha} - \frac{\Gamma}{\hbar} f(h)\rho_0 + \frac{\Gamma}{\hbar}(1 - f(h))\rho_1 \tag{30}$$

$$\frac{\partial \rho_1}{\partial t} = -\sum_\alpha \frac{P_\alpha}{m_\alpha}\frac{\partial \rho_1}{\partial R_\alpha} + \sum_\alpha \frac{\partial \tilde{U}_1}{\partial R_\alpha}\frac{\partial \rho_1}{\partial P_\alpha} + \frac{\Gamma}{\hbar} f(h)\rho_0 - \frac{\Gamma}{\hbar}(1 - f(h))\rho_1 \tag{31}$$

The above equations are what we refer to as a broadened classical master equation (BCME). In Figure 5, we plot the modified potentials $\tilde{U}_0$ and $\tilde{U}_1$. Note that new potentials $\tilde{U}_0$ and $\tilde{U}_1$ approach the original diabatic potentials U_0 and U_1 as well as the true PMF far away from the crossing point. However, the energy where $\tilde{U}_0$ and $\tilde{U}_1$ cross is much lower than the energy where U_0 and U_1 cross, such that the inclusion of broadening will promote hopping with a thermal energy less than the barrier height. One can expect that electron transfer rate between U_0 and U_1 will be larger according to the BCME, as opposed to the CME.

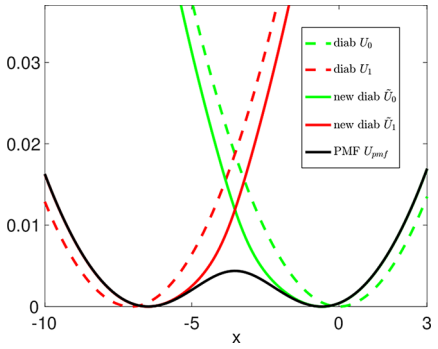

Figure 5. BCME potentials: the new potentials $\tilde{U}_0$ and $\tilde{U}_1$ approach the original diabatic potentials U_0 and U_1 as well as the true PMF far away from the crossing point. At the crossing point, however, the energy where $\tilde{U}_0$ and $\tilde{U}_1$ cross is much lower than the energy where U_0 and U_1 cross, which will result in a larger electron transfer rate.

Overall, the extrapolated BCME in eqs 30 and 31 naturally links the weak molecule−metal interaction regime to the nonadiabatic regime. In the weak molecule−metal interaction regime, broadening effects can be neglected, such that the BCME reduces to the CME. In the nonadiabatic regime, one follows the adiabatic expansion in section 3.2, and maps the BCME onto a FP equation with the corrected broadening (BFP). Therefore, we might expect (or at least hope) that the BCME should work in both the weak and strong coupling regimes as well the adiabatic and nonadiabatic regimes. Note that, in practice, the BCME is easily solved: just for the CME, we simply run classical dynamics on the modified diabatic potentials ($\tilde{U}_0$ and $\tilde{U}_1$), with stochastic hopping between potentials.

Finally, one more word is appropriate vis a vis the notion of broadening. The true electronic friction in eq 15 also contains broadening just like the force in eq 14. Nevertheless, it turns out that the broadening effect for the friction is of higher order in Γ than for the mean force, such that the broadening in friction is less significant than in the mean force. See ref 75. In addition, for classical dynamics, the potential of mean force has a much more significant effect on the dynamics than does friction. For example, in transition state theory, the transition rate decreases exponentially with the increase of the barrier hight of the potential, whereas the transition rate decreases with friction as only $1/\gamma$. Thus, for now, we will simply incorporate broadening only into our potential (and not friction). For very large Γ, broadening in friction may be important, and the broadened friction can be incorporated into BCME as well. See ref 75.

4. KEY NUMERICAL RESULTS

4.1. Electron Transfer Rate.

Obviously, one cannot derive the BCME in eqs 30 and 31 and so empirical testing of BCME dynamics against exact dynamics is crucial. To that end, the most natural test of BCME dynamics is the electron transfer rate, where kinetic theories are available in certain limits. Note that, to apply rate theories, a small external nuclear friction is added to make sure the nuclear DoFs maintain thermal equilibrium. In

https://dx.doi.org/10.1021/acs.jpca.9b10698
J. Phys. Chem. A XXXX, XXX, XXX−XXX

this subsection, the added external nuclear friction is set to be $\gamma_n = 2m\omega$; here ω is the frequency of the nuclear mode and $\gamma_n = 2m\omega$ yields critically damped surface hopping or Langevin dynamics.

In Figure 6, we plot the electron transfer rate as a function of Γ according to BCME and CME dynamics.[99] In the weak molecule−metal interaction regime $\Gamma < kT$, the electron transfer rate from the molecule to the metal is given by Marcus's electrochemical rate constant:[100,101]

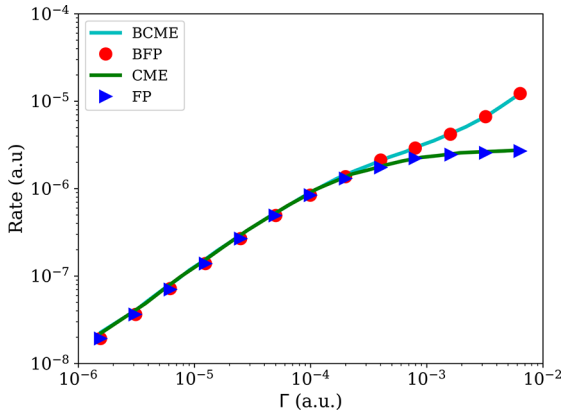

Figure 6. Electron transfer rate at molecule−metal interfaces as a function of molecule−metal interaction Γ according to a broadened classical master equation (BCME), a broadened Fokker−Planck equation (BFP), an ordinary unbroadened classical master equation (CME), and an ordinary unbroadened Fokker−Planck equation (FP). (B)CME reproduces the Marcus electron transfer rate (not shown, but see the agreement in Figure 9 or in ref 98) in the limit of small Γ, where the rates scale linearly with Γ. For large Γ, the electron transfer rate according to BCME and BFP dynamics increases rapidly with Γ, due to a lowering of the energy barrier; by contrast, the CME and FP rates are independent of Γ. Suprisingly, (B)FP reproduces the (B)CME rate (or Marcus rate) in the nonadiabatic regime, i.e., small Γ. See the discussion in the main text.

$$k_{\text{Marcus}} = \int \frac{\Gamma}{\hbar}(1 - f(E))\frac{e^{-(E_r - \bar{\epsilon}_d + E)}}{\sqrt{4\pi E_r kT}}\, dE \tag{32}$$

Note that, by averaging the usual (Marcus) homogeneous electron transfer rates over a continuum of electronic states, the above equation takes into account the plethora of metallic states that can accept the molecular electron. Note also that, in this regime, the electron transfer rate scales linearly with Γ. As Figure 9 demonstrates, the BCME and CME can reproduce the Marcus rate in this limit; the Marcus rate is not shown here, but see the agreement in Figure 9 or in ref 98. In ref 38, we further prove analytically that the BCME and CME electron transfer rates agree with the Marcus rate in the small Γ limit.

For intermediate molecule−metal couplings, $\hbar\omega < \Gamma < kT$, Figure 6 also shows that surface hopping dynamics are equivalent to Langevin dynamics, such that the (B)CME and (B)FP quantitively agree and adiabatic transition state theory can be applied. According to adiabatic transition state theory, for intermediate values of Γ, broadening effects are not significant; electron friction deceases with Γ but is overpowered by nuclear friction, such that the electron transfer rate is independent of Γ.

Finally, when Γ gets even larger, $\Gamma > kT$, the dynamics remain adiabatic and transition state theory should still apply. However, as Figure 6 shows, broadening effects are now crucial and show strong signatures as a result of lowering the potential energy barrier. According to transition state theory, lowering this energy barrier should exponentially increase the electron transfer rate, and indeed we find that, in this regime, the electron transfer rate according to BFP and BCME dynamics grows rapidly with Γ. That being said, according to CME and FP dynamics, broadening effects are neglected, such that in Figure 6, the CME and FP electron current (erroneously) remain constant regardless of Γ.

One observation from Figure 6 is surprising: In the limit of small Γ, the electron transfer rate according to the (B)FP agrees with (B)CME. As stated in section 3.2, in principle, the (B)FP equation of motion should be valid only in the adiabatic limit, i.e., for intermediate and large Γ. After all, electronic friction (eq 23) diverges with very small Γ. Interestingly, this feature seems to incorporate some of the correct physics in practice. In ref 98, using transition state theory, we prove that electronic friction-Langevin dynamics can actually reproduce the Marcus rate in the small Γ limit. Of course, this agreement is true only under certain conditions, e.g., a large barrier and a one-dimensional crossing, and even then electronic friction is certainly not always reliable in the strong nonadiabatic regime; for example, see the case of nuclear relaxation in Figure 4. In ref 102, we further explore the case of multiple dimensional crossings, which highlights a bit more carefully when electronic friction is reliable for electron transfer near a metal surface.

4.2. Out of Equilibrium: *I*−*V* Curves and Heating Effects. To further test BCME dynamics, we have benchmarked the BCME against numerically exact solutions using the hierarchical master equation (HQME) for transport properties. Whereas the above discussion centered around the case of one metal, i.e., the equilibrium case, we now consider a molecule connected to two metals with unequal Fermi energies and subject to nonequilibrium electronic currents. The extension of CME or BCME dynamics to this nonequilibrium case can be easily realized by adding another hopping term due to couplings to the second metal. Within the BCME, transport properties can be evaluated by averaging the corresponding local observables over nuclear distributions. For instance, the total current is given by

$$I = \int I_{\text{loc}}(x)(\rho_0(x,p) + \rho_1(x,p))\, dx\, dp \tag{33}$$

where $I_{\text{loc}}(x)$ is the local current given by

$$I_{\text{loc}} = \frac{e}{\hbar}\int \frac{d\epsilon}{2\pi}\frac{\Gamma_L\Gamma_R}{(\epsilon - h(x))^2 + (\Gamma_L + \Gamma_R)^2/4}(f^L(\epsilon) - f^R(\epsilon)) \tag{34}$$

See ref 76 for details.

In Figure 7, we plot the electronic current as a function of electron voltage. We note that the BCME agrees with the HQME almost exactly, whereas the unbroadened CME fails when we increase Γ. The *I*−*V* curves from the unbroadened CME have sharper features regardless of Γ, which is a consequence of neglecting broadening; broadening tends to decrease the electronic current as been captured by the BCME. In this regime of classical nuclear motion, the CME also reproduces the quantum master equation (QME) solution. See ref 76 for details about the quantum mechanical treatment of nuclear motion and how to incorporate broadening within a fully quantum QME (bQME).

Lastly, as far as nuclear dynamics are concerned, in Figure 8, we plot the phonon population as a function of electron voltage. Again, the BCME agrees with the HQME almost exactly for all

https://dx.doi.org/10.1021/acs.jpca.9b10698
J. Phys. Chem. A XXXX, XXX, XXX−XXX

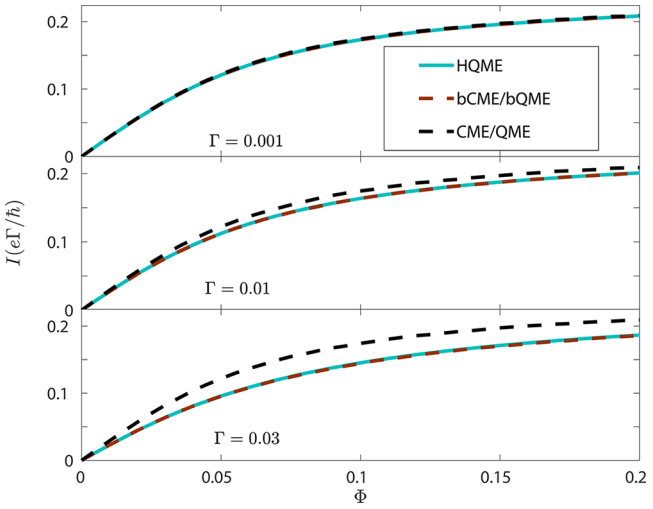

Figure 7. *IV* curves. The CME agrees with numerically exact results from HQME for small Γ; for large Γ, *I*−*V* curves from the CME yield features that are too sharp due to a lack of broadening. By contrast, the BCME agrees with the HQME almost exactly. The QME includes a fully quantum mechanical treatment of nuclear motion, which agrees with the CME in this classical regime ($kT > \hbar\omega$). See also ref 76 for a detailed discussion of QME dynamics and how to incorporate broadening within the QME framework (yielding a bQME).

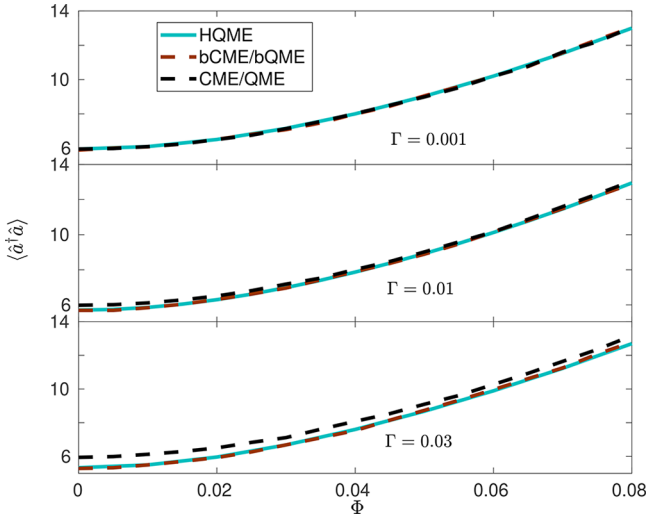

Figure 8. Phonon population as a function of voltage. The BCME reproduces the numerically exact results from the HQME, whereas the CME works only in the small Γ case regime. The phonon population increases dramatically with voltage bias, leading to instability of the molecular junction. See also ref 76 for a detailed discussion of QME dynamics and how to incorporate broadening within the QME framework (yielding a bQME).

Γ, whereas the CME works only in the small Γ regime. Note that, at zero bias, when Γ gets large, the phonon population from the BCME decreases, which is consistent with the lowering of the potential of mean force energy barrier. The CME fails to reproduce these features, again due to a lack of broadening. Note also that the phonon population increases dramatically with the voltage bias. Obviously, with a nonzero electronic voltage across the system, nuclei do not remain in thermal equilibrium any more; rather, the electronic current heats up the vibrational DoFs of the molecule, which can lead to instability of the molecular junction.[36,103−105]

4.3. IESH vs BCME. As noted in the Introduction, the Shenvi−Roy−Tully IESH framework was the first surface hopping algorithm to study nonadiabatic dynamics near a metal surface. Beyond the usual assumptions of the FSSH algorithm, two additional approximations are notable within IESH: (1) Instead of tracing out the electronic DoFs in the metal (as done above), IESH discretizes the continuum of the metal, and a finite number of electronic levels are chosen, usually up to around 90 levels as limited by the high computational cost. (2) Only single excitations are allowed at each time step within IESH. Despite these approximations, IESH does partially reproduce experimental studies of energy relaxation for NO on a gold surface;[71] however, until recently, the general validity of IESH was not fully tested or benchmarked over a large set of different parameter regimes. In ref 72, we have now made such a comparison, testing IESH versus both BCME and Marcus theory.

In Figure 9, we plot the electron transfer rate as a function of Γ for both IESH and BCME. As stated above, both BCME and

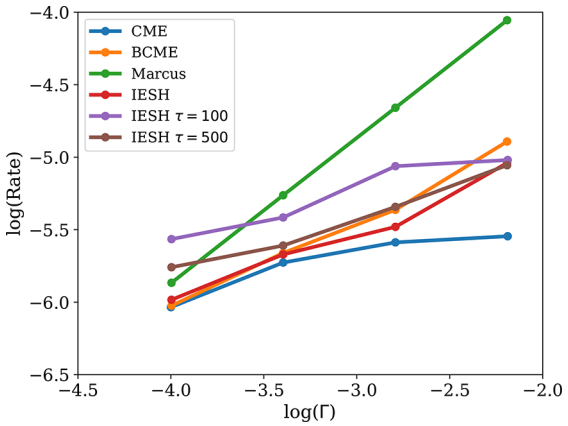

Figure 9. Electron transfer rate as a function of Γ. The BCME and CME reproduce the Marcus rate for small Γ. When Γ gets larger, the CME rate (incorrectly) levels off, whereas the BCME rate increase rapidly with Γ. IESH results agree with BCME results in general. Here τ for IESH represents an electronic thermostat, which should help to mimic an open quantum system. Unfortunately, however, we find that adding such an electronic thermostat apparently can make the dynamics worse.[72]

CME reproduce the Marcus rate for small Γ. When Γ gets larger, the CME rate levels off (erroneously), whereas the BCME rate increases rapidly with Γ. IESH does agree with the BCME in general. Note that, for IESH, since the metal is treated as a closed system, the electronic temperature is missing. To partly address this issue, inclusion of an electronic thermostat has been suggested,[106] and τ represents the time scale for an electronic thermostat in Figure 9. Unfortunately, according to Figure 9, we find that adding such an electronic thermostat can make the coupled nuclear-electronic dynamics worse. That being said, adding such an electronic thermostat can help IESH to recover the correct equilibrium; without such a thermostat, equilibrium solutions from IESH can be incorrect. See discussion in ref 72 for details.

In conclusion, treating the electronic DoFs from the metal surface explicitly as is done with IESH is a bit tricky. As a huge plus, no assumption regarding the molecule−metal couplings (e.g., wide band approximation, weak coupling) are needed. As a minus, however, such a treatment is expensive, the dynamics can

https://dx.doi.org/10.1021/acs.jpca.9b10698
J. Phys. Chem. A XXXX, XXX, XXX−XXX

be hard to converge, and adding a thermostat can fix one problem (equilibrium populations) but lead to other problems (worse dynamics). The optimal means to incorporate a thermostat needs to be investigated in the future. Finally, is there a way to push IESH to the nonequilibrium case to study transport properties? This remains an open question.

5. MOLECULE WITH MULTIPLE LEVELS: QCLE-CME

Our discussion above has been restricted to the AH model, where a single level in the molecule is hybridized with the electronic DoFs in the metal. When mimicking a realistic molecule with *many* electronic orbitals coupled to a metal surface, one must generalize the relevant equations of motion for coupled electron−nuclear dynamics.

To be specific, let us consider a molecule with multiple electronic levels ($\hat{d}_m$) coupled to a set of nuclear DoFs:

$$\hat{H}_s = \sum_{mn} h_{mn}\hat{d}_m^+\hat{d}_n + U_0(\mathbf{R}) + \sum_\alpha \frac{P_\alpha^2}{2m_\alpha} \tag{35}$$

Here h_{mn} is interaction energy between level $\hat{d}_m$ and $\hat{d}_n$ in the molecule. The couplings between the molecule and metal also have to be generalized

$$\hat{H}_I = \sum_{mk} V_{mk}(\hat{d}_m^+\hat{c}_k + \hat{c}_k^+\hat{d}_m) \tag{36}$$

Here V_{mk} is the coupling energy between the molecular $\hat{d}_m$ level and metallic k level. The Hamiltonian for the metal remains the same as the one in eq 3.

As for the case of a single molecular level, we focus on the mixed quantum classical density of the molecule, and we trace out the electronic DoFs in the metal. By treating the interactions between the molecule and metal pertubatively up to second order, provided the nuclear motion can be treated classically, we arrive at a quantum-classical Liouville equation embedded into a classical master equation (QCLE-CME):[92,107]

$$\frac{\partial}{\partial t}\hat{\rho}(\mathbf{R},\mathbf{P},t) = -\sum_\alpha \frac{P_\alpha}{m_\alpha}\frac{\partial\hat{\rho}}{\partial R_\alpha} + \frac{1}{2}\sum_\alpha\left(\frac{\partial\hat{H}_s}{\partial R_\alpha}\frac{\partial\hat{\rho}}{\partial P_\alpha} + \frac{\partial\hat{\rho}}{\partial P_\alpha}\frac{\partial\hat{H}_s}{\partial R_\alpha}\right) - \frac{i}{\hbar}[\hat{H}_s,\hat{\rho}] - \hat{\hat{\mathcal{L}}}\hat{\rho} \tag{37}$$

Here $\hat{\rho}(\mathbf{R},\mathbf{P},t)$ is the density operator in phase space ($\mathbf{R}$, $\mathbf{P}$) at time t. The first three terms on the right-hand side of eq 37 are the standard QCLE,[19,95] describing nonadiabatic dynamics for an isolated molecule;[94] the super operator $\hat{\hat{\mathcal{L}}}$ as found in the last term takes into account the molecule−metal interaction, describing electron transfer between the molecule and metal. The exact form of this super operator can be found in refs 92 and 107. Of course, in the case of one electronic level considered in the molecule, the QCLE-CME in eq 37 reduces to the CME in eqs 6 and 7.

Now in section 3.1, we demonstrated that there is a natural surface hopping solution to the CME. Moreover, in refs 19, 89, 108, and 109 two different groups have demonstrated a connection between the QCLE and Tully's FSSH. Thus, one might expect that one can fashion a hybridized scheme Tully/CME surface hopping scheme to solve the QCLE-CME. To that end, because Tully's surface hopping algorithm can be understood naturally only in an adiabatic representation, one must transform the QCLE-CME into the adiabatic representation. The adiabatic representation of the QCLE-CME can be found in ref 92. With such an adiabatic representation, it is clear that hopping between two quantum states can be induced by two distinct mechanisms: (1) nuclear motion as incorporated by derivative couplings and (2) electronic dynamics between molecule and metal as incorporated by molecule−metal couplings. For the first mechanism, the nonadiabatic dynamics as induced by derivative couplings are naturally introduced in the QCLE part and can be addressed with Tully's FSSH. These dynamics can give rise to electron transfer within the molecule (i.e., they should preserve the electronic population of the quantum subsystem). Second, the nonadiabatic dynamics arising from molecule−metal couplings are captured by the super operator $\hat{\hat{\mathcal{L}}}$, which gives rise to electron transfer between the molecule and metal and can be addressed with CME-like surface hops. Note that, unlike the single level case (eqs 6 and 7), where molecular populations do not couple to molecular coherences, in the case of multiple electronic states, populations do couple to coherences through the super operator $\hat{\hat{\mathcal{L}}}$. As such, there is no absolutely clean means to decouple these two distinct dynamical mechanisms and, as such, tricky coherence/decoherence issue can arise—more so than in the case for Tully's FSSH algorithm for which we do now have a fairly accurate understanding of and treatment for decoherence.[23−25,89−91,110]

In Figure 10, we present results for a series of different QCLE-CME surface hopping schemes as benchmarked against a quantum master equation for a donor−acceptor−metal model

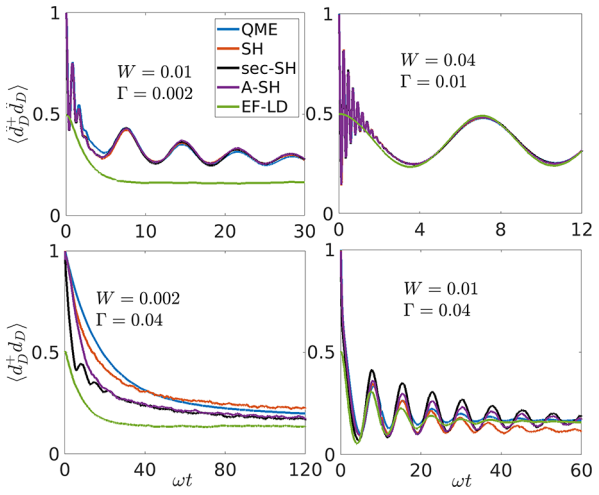

Figure 10. We plot electron population on the donor for a donor−acceptor−metal model. W is the diabatic coupling between donor and acceptor, and Γ is the hybridization function between the acceptor and metal. See eqs 38,39, and 5. Here the QME can be viewed as an exact solution. Surface hopping dynamics with or without decoherence agree with QME well in the case of $W > \Gamma$ (upper two panels). In the case of small W compared to Γ (lower two panels), SH dynamics without decoherence leads to the wrong equilibrium states. Ignoring coherence completely (sec-SH) can recover the correct equilibrium solution, but at the cost of dynamics with larger errors. An augmented SH solution with decoherence correctness (A-SH) works well for both dynamics and equilibrium states, but the decoherence problem is far more complicated near a metal as compared to in solution, and far more research is needed in this area. Electronic friction-Langevin dynamics (EF-LD) only work for both large W and Γ (right two panels), i.e., adiabatic limit. In addition, EF-LD misses all oscillations and initial conditions in electronic dynamics at short times.

https://dx.doi.org/10.1021/acs.jpca.9b10698
J. Phys. Chem. A XXXX, XXX, XXX−XXX

(with four quantum states). The system Hamiltonian (donor−acceptor part with a nuclear DoF) is

$$\hat{H}_s = E_D(x)\hat{d}_D^+\hat{d}_D + E_A(x)\hat{d}_A^+\hat{d}_A + W(\hat{d}_A^+\hat{d}_D + \hat{d}_D^+\hat{d}_A) + \frac{1}{2}m\omega x^2 + \frac{p^2}{2m} \quad (38)$$

Here W is the coupling energy between the donor and acceptor. The acceptor states linearly couple to the metal states

$$\hat{H}_I = \sum_k V_k(\hat{d}_A^+\hat{c}_k + \hat{c}_k^+\hat{d}_A) \quad (39)$$

Again, we will use Γ (see eq 5) to quantify the strength of acceptor−metal coupling. For weak acceptor−metal coupling, the QME can be viewed as an exact solution. In such a model, an electron can be transferred between donor and acceptor as well as between acceptor and metal surface. In the figure, the curve "SH" does include any additional decoherence. "A-SH" represents an augmented surface hopping algorithm that incorporates decoherence in a similar fashion as A-FSSH includes decoherence on top of Tully's FSSH.[24] "Sec-SH" signifies the secular approximation, whereby coherence between different adiabatic states of the molecular system is completely ignored. In the adiabatic limit, following a similar procedure in section 3.2, the QCLE-CME can be mapped onto a FP equation as well. The resulting friction can be found in ref 107.

As shown in the upper two panels of Figure 10, when the coupling between the donor and acceptor is not weak compared to acceptor−metal coupling ($W > \Gamma$), and when decoherence is not an issue, all surface hopping algorithms (with or without decoherence) work well for both electronic dynamics and nuclear dynamics as compared to QME; by contrast, electronic friction-Langevin dynamics is meaningful only for larger W and Γ. See eqs 38, 39, and 5 for a definition of W and Γ. To be specific, for such a model, the time scales for electronic dynamics are limited by the donor−acceptor couplings W and the acceptor−metal couplings Γ, such that electronic friction-Langevin dynamics work only when W and Γ are both large. In addition, EF-LD misses all oscillations in electronic dynamics at short times.

Despite the highly encouraging results above, when the donor−acceptor coupling is weak compared to acceptor−metal coupling ($W < \Gamma$) and one is strongly breaking the Born−Oppenheimer approximation, decoherence will matter and the dynamics become more difficult to solve. In the lower two panels of Figure 10, we show that errors in capturing decoherence (in SH) can eventually lead to the wrong equilibrium states. Vice versa, if we ignore coherence completely (sec-SH), we can recover the correct equilibrium solution, but at the cost of dynamics with larger errors (as compared with the exact solution). Overall, a decoherence-corrected SH algorithm (A-SH in Figure 10) works best compared to the other methods, but much more work in this area (and with larger Hamiltonians and with different approaches to capture decoherence) will be necessary in the future.

6. OPEN QUESTIONS

Having reviewed our general findings for molecular dynamics on metal surfaces, we should now highlight that many open questions remain before the methods discussed above can be truly predictive for big, realistic (and ideally *ab initio*) systems. The results above were fairly exhaustive for the case of a single electronic (impurity) level near a surface, but many questions remain when there are many relevant quantum states, quantum (as opposed to classical) nuclear motion, and strong electron−electron interactions.

6.1. Broadening within the QCLE-CME. Just like the CME in eqs 6 and 7 (for two quantum states), the QCLE-CME in eq 37 (for many quantum states) is derived by assuming the presence of relatively weak molecule−metal interaction and thus ignores all broadening effects as well. Just as for the case of the BCME, one natural way to incorporate broadening effects within the QCLE-CME would be to simply modify the relevant potentials. While we have preliminary results showing that such an idea can work well in certain regimes, future tests are required to fully benchmark the weakness and strength of such a broadening scheme within the QCLE-CME framework.

Another question regarding the QCLE-CME is the decoherence problem. In the presence of a metal surface, an electronic bath introduces decoherence naturally beyond the usual decoherence as introduced by opposite forces leading to different nuclear motion on different electronic surfaces.[24,25,27,90,110−119] Are these two decoherence mechanisms entirely decoupled? Can they be added together? This is a very tricky question, and anomalous results can be obtained if one is not careful to be sure that detailed balance is correctly achieved.[92] Understanding the balance of coherence versus decoherence—for a molecule with a metallic environment on one side and a solvated environment on the other—is a key question for future research on electrochemical systems.

6.2. Nuclear Quantum Effects. To date, we have mostly treated nuclear motion classically, but for high frequency modes, nuclear quantum effects can obviously be important. Currently, there is a big push to incorporate the nuclear quantum effect in molecular dynamics both in the gas phase and in solution, adiabatically and nonadiabatically using ring polymer approaches.[120−130] While moving ring polymers on different surfaces is a complicated task (do the beads move collectively or independently?), one very interesting feature of dynamics near metal surfaces is the isomorphism between hopping and frictional approaches,[74,75] as appropriate when the molecule−metal coupling Γ is not too big or too small. It will be very interesting to see if one can derive (or even guess) a nonadiabatic approach for dynamics near metal surfaces that preserves this isomorphism.

6.3. Electron−Electron Interaction in Nonadiabatic Dynamics. Finally, at this point, the most important question not yet discussed is how to actually describe the electronic states of the molecule, the electronic states of the metal, and the molecule−metal interactions. According to eqs 1−4, we have neglected electron−electron (el−el) interactions and focused exclusively on coupled nuclear-electronic problems. Thus, two immediate questions arise: First, if we want to use eqs 1−4, what is the best means to parametrize such a model of noninteracting electronic states using a practical electronic structure theory method, e.g., DFT? Surely, we should borrow from the large and relevant literature for molecular conduction,[51,101,131−133] but we should also keep in mind that we require smooth parametrizations for many different nuclear geometries.

Second, it is not yet clear exactly what features do we miss by ignoring electron−electron interactions when solving for nuclear-electronic dynamics, and how important are those features? In refs 46 and 47, for the interacting AH model with electron−electron repulsion, we showed that including el−el interactions not only changes potential energy surfaces (which is

https://dx.doi.org/10.1021/acs.jpca.9b10698
J. Phys. Chem. A XXXX, XXX, XXX−XXX

obvious) but also gives rise to interesting resonances and new exotic peaks in the electronic friction profile (which is not obvious). For larger molecules, will the effects of electron−electron interactions be similar? And most importantly, are there experimental signatures of an exotic electron friction tensor, or are all friction effects necessarily smeared away in practice by the presence of a distribution of velocities? With better treatment of el−el interaction from electronic structure theory, one would hope to answer some of these questions in the future.

7. CONCLUSIONS

The study of dynamics at a metal surface is an enormous problem in chemical and condensed matter physics, and this Feature Article has made no attempt to be (even close to) exhaustive. Instead of reviewing the enormous literature,[69,77−81] we have attempted to summarize our recent experiences with semiclassical models of such dynamics, whereby classical nuclear motion is entangled with quantum electronic motion. We have shown that quite a bit of progress has been made for model problems, such that we now have a reasonably accurate conceptual picture of dynamics near metal surfaces: one can adapt either a hopping or frictional perspective and one can successfully interpolate between the two. Furthermore, for model problems, one can make phenomenological predictions given a set of reasonable parameters capturing the molecule, metal, and molecule−metal interactions. Nevertheless, as highlighted in the last section, many obstacles remain before these methods can be predictive for realistic systems, especially with regard to electron−electron interactions; for researchers interested in the intersection of electronic structure theory and quantum dynamics, now is clearly a great time to be working on molecule−metal surface dynamics.

AUTHOR INFORMATION

Corresponding Authors

Wenjie Dou − *Department of Chemistry, University of California, Berkeley, Berkeley, California 94720, United States;* orcid.org/0000-0001-5410-6183; Email: douw@berkeley.edu

Joseph E. Subotnik − *Department of Chemistry, University of Pennsylvania, Philadelphia, Pennsylvania 19104, United States;* Email: subotnik@sas.upenn.edu

Complete contact information is available at: https://pubs.acs.org/10.1021/acs.jpca.9b10698

Notes

The authors declare no competing financial interest.

Biographies

Wenjie Dou is a postdoctoral researcher at University of California, Berkeley. He got his B.S. in physics from University of Science and Technology of China in 2013 and Ph.D. in chemistry with Joseph Subotnik at the University of Pennsylvania in 2018. His Ph.D. work focused on modeling non-adiabatic dynamics near metal surfaces. He currently works with Eran Rabani on stochastic implementation of electronic structure theory for excited states.

Joseph Subotnik is a Professor at the University of Pennsylvania. He earned a B.A. in physics and math from Harvard University in 2000 and a Ph.D. in biophysics with Martin Head-GOrdon at Berkeley. As a postdoctoral fellow, he worked with Abe Nitzan (Tel-Aviv University) and Mark Ratner (Northwestern University). His research interests are modeling how charge and energy flow through materials, with a special focus on non-adiabatic phenomena.

ACKNOWLEDGMENTS

This work was supported by the (U.S.) Air Force Office of Scientific Research (USAFOSR) under AFOSR Grants No. FA9950-18-1-0420 and FA9950-18-1-0497.

REFERENCES

(1) Krüger, B. C.; Meyer, S.; Kandratsenka, A.; Wodtke, A. M.; Schäfer, T. Vibrational Inelasticity of Highly Vibrationally Excited NO on Ag (111). *J. Phys. Chem. Lett.* **2016**, *7*, 441−446.

(2) Huang, Y.; Rettner, C. T.; Auerbach, D. J.; Wodtke, A. M. Vibrational Promotion of Electron Transfer. *Science* **2000**, *290*, 111−114.

(3) Bünermann, O.; Jiang, H.; Dorenkamp, Y.; Kandratsenka, A.; Janke, S. M.; Auerbach, D. J.; Wodtke, A. M. Electron-hole pair excitation determines the mechanism of hydrogen atom adsorption. *Science* **2015**, *350*, 1346−1349.

(4) Brandbyge, M.; Hedegård, P.; Heinz, T. F.; Misewich, J. A.; Newns, D. M. Electronically driven adsorbate excitation mechanism in femtosecond-pulse laser desorption. *Phys. Rev. B: Condens. Matter Mater. Phys.* **1995**, *52*, 6042−6056.

(5) Ouyang, W.; Saven, J. G.; Subotnik, J. E. A Surface Hopping View of Electrochemistry: Non-Equilibrium Electronic Transport through an Ionic Solution with a Classical Master Equation. *J. Phys. Chem. C* **2015**, *119*, 20833−20844.

(6) Hammes-Schiffer, S.; Soudackov, A. V. Proton-coupled electron transfer in solution, proteins, and electrochemistry. *J. Phys. Chem. B* **2008**, *112*, 14108−14123.

(7) Persson, B. Applications of surface resistivity to atomic scale friction, to the migration of "hot" adatoms, and to electrochemistry. *J. Chem. Phys.* **1993**, *98*, 1659−1672.

(8) Mohr, J.-H.; Schmickler, W. Exactly Solvable Quantum Model for Electrochemical Electron-Transfer Reactions. *Phys. Rev. Lett.* **2000**, *84*, 1051.

(9) Luo, X.; Jiang, B.; Juaristi, J. I.; Alducin, M.; Guo, H. Electron-hole pair effects in methane dissociative chemisorption on Ni (111). *J. Chem. Phys.* **2016**, *145*, 044704.

(10) Luntz, A. In *Chemical Bonding at Surfaces and Interfaces*; Nilsson, A., Pettersson, L. G., Norskov, J. K., Eds.; Elsevier: Amsterdam, 2008; pp 143−254.

(11) Luntz, A.; Persson, M.; Wagner, S.; Frischkorn, C.; Wolf, M. Femtosecond laser induced associative desorption of H2 from Ru (0001): Comparison of first principles theory with experiment. *J. Chem. Phys.* **2006**, *124*, 244702.

(12) Nitzan, A.; Ratner, M. A. Electron transport in molecular wire junctions. *Science* **2003**, *300*, 1384.

(13) Galperin, M.; Ratner, M. A.; Nitzan, A.; Troisi, A. Nuclear Coupling and Polarization in Molecular Transport Junctions: Beyond Tunneling to Function. *Science* **2008**, *319*, 1056.

(14) Shi, Q.; Geva, E. A new approach to calculating the memory kernel of the generalized quantum master equation for an arbitrary system-bath coupling. *J. Chem. Phys.* **2003**, *119*, 12063.

(15) Kelly, A.; Brackbill, N.; Markland, T. E. Accurate nonadiabatic quantum dynamics on the cheap: Making the most of mean field theory with master equations. *J. Chem. Phys.* **2015**, *142*, 094110.

(16) Meyer, H.-D.; Miller, W. H. A classical analog for electronic degrees of freedom in nonadiabatic collision processes. *J. Chem. Phys.* **1979**, *70*, 3214.

(17) Stock, G.; Thoss, M. Semiclassical Description of Nonadiabatic Quantum Dynamics. *Phys. Rev. Lett.* **1997**, *78*, 578.

(18) Liu, J. Isomorphism between the multi-state Hamiltonian and the second-quantized many-electron Hamiltonian with only 1-electron interactions. *J. Chem. Phys.* **2017**, *146*, 024110.

(19) Kapral, R.; Ciccotti, G. Mixed quantum-classical dynamics. *J. Chem. Phys.* **1999**, *110*, 8919.

(20) Huo, P.; Coker, D. F. Consistent schemes for non-adiabatic dynamics derived from partial linearized density matrix propagation. *J. Chem. Phys.* **2012**, *137*, 22A535.

(21) Ben-Nun, M.; Martinez, T. J. Nonadiabatic molecular dynamics: Validation of the multiple spawning method for a multidimensional problem. *J. Chem. Phys.* **1998**, *108*, 7244.
(22) Min, S. K.; Agostini, F.; Gross, E. K. U. Coupled-Trajectory Quantum-Classical Approach to Electronic Decoherence in Non-adiabatic Processes. *Phys. Rev. Lett.* **2015**, *115*, 073001.
(23) Tully, J. C. Molecular dynamics with electronic transitions. *J. Chem. Phys.* **1990**, *93*, 1061−1071.
(24) Landry, B. R.; Subotnik, J. E. How to recover Marcus theory with fewest switches surface hopping: Add just a touch of decoherence. *J. Chem. Phys.* **2012**, *137*, 22A513.
(25) Prezhdo, O. V.; Rossky, P. J. Mean-field molecular dynamics with surface hopping. *J. Chem. Phys.* **1997**, *107*, 825.
(26) Bellonzi, N.; Jain, A.; Subotnik, J. E. An assessment of mean-field mixed semiclassical approaches: Equilibrium population and algorithm stability. *J. Chem. Phys.* **2016**, *144*, 154110.
(27) Fang, J.-Y.; Hammes-Schiffer, S. Comparison of surface hopping and mean field approaches for model proton transfer reactions. *J. Chem. Phys.* **1999**, *110*, 11166.
(28) Casanova, D. Theoretical Modeling of Singlet Fission. *Chem. Rev.* **2018**, *118*, 7164−7207.
(29) Tempelaar, R.; van der Vegte, C. P.; Knoester, J.; Jansen, T. L. C. Surface hopping modeling of two-dimensional spectra. *J. Chem. Phys.* **2013**, *138*, 164106.
(30) Petit, A. S.; Subotnik, J. E. How to calculate linear absorption spectra with lifetime broadening using fewest switches surface hopping trajectories: A simple generalization of ground-state Kubo theory. *J. Chem. Phys.* **2014**, *141*, 014107.
(31) Chen, H.-T.; Li, T. E.; Sukharev, M.; Nitzan, A.; Subotnik, J. E. Ehrenfest+ R dynamics. II. A semiclassical QED framework for Raman scattering. *J. Chem. Phys.* **2019**, *150*, 044103.
(32) Thoss, M.; Kondov, I.; Wang, H. Correlated electron-nuclear dynamics in ultrafast photoinduced electron-transfer reactions at dye-semiconductor interfaces. *Phys. Rev. B: Condens. Matter Mater. Phys.* **2007**, *76*, 153313.
(33) Mühlbacher, L.; Rabani, E. Real-Time Path Integral Approach to Nonequilibrium Many-Body Quantum Systems. *Phys. Rev. Lett.* **2008**, *100*, 176403.
(34) Schinabeck, C.; Erpenbeck, A.; Härtle, R.; Thoss, M. Hierarchical quantum master equation approach to electronic-vibrational coupling in nonequilibrium transport through nanosystems. *Phys. Rev. B: Condens. Matter Mater. Phys.* **2016**, *94*, 201407.
(35) Xu, M.; Liu, Y.; Song, K.; Shi, Q. A non-perturbative approach to simulate heterogeneous electron transfer dynamics: Effective mode treatment of the continuum electronic states. *J. Chem. Phys.* **2019**, *150*, 044109.
(36) Härtle, R.; Thoss, M. Vibrational instabilities in resonant electron transport through single-molecule junctions. *Phys. Rev. B: Condens. Matter Mater. Phys.* **2011**, *83*, 125419.
(37) Koch, J.; von Oppen, F.; Oreg, Y.; Sela, E. Thermopower of single-molecule devices. *Phys. Rev. B: Condens. Matter Mater. Phys.* **2004**, *70*, 195107.
(38) Dou, W.; Nitzan, A.; Subotnik, J. E. Surface hopping with a manifold of electronic states, III: transients, broadening and the Marcus picture. *J. Chem. Phys.* **2015**, *142*, 234106.
(39) Bruch, A.; Lewenkopf, C.; von Oppen, F. Landauer-Büttiker Approach to Strongly Coupled Quantum Thermodynamics: Inside-Outside Duality of Entropy Evolution. *Phys. Rev. Lett.* **2018**, *120*, 107701.
(40) Bode, N.; Kusminskiy, S. V.; Egger, R.; von Oppen, F. Current-induced forces in mesoscopic systems: A scattering-matrix approach. *Beilstein J. Nanotechnol.* **2012**, *3*, 144.
(41) Kershaw, V. F.; Kosov, D. S. Nonequilibrium GreenâĂŹs function theory for nonadiabatic effects in quantum electron transport. *J. Chem. Phys.* **2017**, *147*, 224109.
(42) Chen, H.-T.; Cohen, G.; Millis, A. J.; Reichman, D. R. Anderson-Holstein model in two flavors of the noncrossing approximation. *Phys. Rev. B: Condens. Matter Mater. Phys.* **2016**, *93*, 174309.
(43) Galperin, M.; Ratner, M. A.; Nitzan, A. Molecular transport junctions: vibrational effects. *J. Phys.: Condens. Matter* **2007**, *19*, 103201.
(44) Haug, H.; Jauho, A. *Quantum Kinetics in Transport and Optics of Semiconductors*.; Springer: New York, 2007.
(45) Chen, F.; Miwa, K.; Galperin, M. Current-induced forces for nonadiabatic molecular dynamics. *J. Phys. Chem. A* **2019**, *123*, 693−701.
(46) Dou, W.; Miao, G.; Subotnik, J. E. Born-Oppenheimer Dynamics, Electronic Friction, and the Inclusion of Electron-Electron Interactions. *Phys. Rev. Lett.* **2017**, *119*, 046001.
(47) Dou, W.; Subotnik, J. E. Perspective: How to understand electronic friction. *J. Chem. Phys.* **2018**, *148*, 230901.
(48) Smith, B. B.; Hynes, J. T. Electronic friction and electron transfer rates at metallic electrodes. *J. Chem. Phys.* **1993**, *99*, 6517−6530.
(49) Persson, B.; Persson, M. Vibrational lifetime for CO adsorbed on Cu(100). *Solid State Commun.* **1980**, *36*, 175−179.
(50) d'Agliano, E. G.; Kumar, P.; Schaich, W.; Suhl, H. Brownian motion model of the interactions between chemical species and metallic electrons: Bootstrap derivation and parameter evaluation. *Phys. Rev. B* **1975**, *11*, 2122−2143.
(51) Lü, J.-T.; Brandbyge, M.; Hedegård, P.; Todorov, T. N.; Dundas, D. Current-induced atomic dynamics, instabilities, and Raman signals: Quasiclassical Langevin equation approach. *Phys. Rev. B: Condens. Matter Mater. Phys.* **2012**, *85*, 245444.
(52) Daligault, J.; Mozyrsky, D. Ion dynamics and energy relaxation rate in nonequilibrium electron-ion systems. *Phys. Rev. E* **2007**, *75*, 026402.
(53) Head-Gordon, M.; Tully, J. C. Molecular dynamics with electronic frictions. *J. Chem. Phys.* **1995**, *103*, 10137.
(54) Struck, L. M.; Richter, L. J.; Buntin, S. A.; Cavanagh, R. R.; Stephenson, J. C. Femtosecond Laser-Induced Desorption of CO from Cu(100): Comparison of Theory and Experiment. *Phys. Rev. Lett.* **1996**, *77*, 4576.
(55) Prybyla, J. A.; Tom, H. W. K.; Aumiller, G. D. Femtosecond time-resolved surface reaction: Desorption of Co from Cu(111) in <325 fsec. *Phys. Rev. Lett.* **1992**, *68*, 503.
(56) Füchsel, G.; Klamroth, T.; Montureta, S.; Saalfrank, P. Dissipative dynamics within the electronic friction approach: the femtosecond laser desorption of H2/D2 from Ru(0001). *Phys. Chem. Chem. Phys.* **2011**, *13*, 8659.
(57) Persson, M.; Hellsing, B. Electronic Damping of Adsorbate Vibrations on Metal Surfaces. *Phys. Rev. Lett.* **1982**, *49*, 662−665.
(58) Hellsing, B.; Persson, M. Electronic damping of atomic and molecular vibrations at metal surfaces. *Phys. Scr.* **1984**, *29*, 360.
(59) Rittmeyer, S. P.; Meyer, J.; Juaristi, J. I. n.; Reuter, K. Electronic Friction-Based Vibrational Lifetimes of Molecular Adsorbates: Beyond the Independent-Atom Approximation. *Phys. Rev. Lett.* **2015**, *115*, 046102.
(60) Maurer, R. J.; Askerka, M.; Batista, V. S.; Tully, J. C. Ab initio tensorial electronic friction for molecules on metal surfaces: Non-adiabatic vibrational relaxation. *Phys. Rev. B: Condens. Matter Mater. Phys.* **2016**, *94*, 115432.
(61) Spiering, P.; Meyer, J. Testing Electronic Friction Models: Vibrational De-excitation in Scattering of H2 and D2 from Cu (111). *J. Phys. Chem. Lett.* **2018**, *9*, 1803.
(62) Kroes, G.-J.; Juaristi, J. I.; Alducin, M. Vibrational Excitation of H2 Scattering from Cu(111): Effects of Surface Temperature and of Allowing Energy Exchange with the Surface. *J. Phys. Chem. C* **2017**, *121*, 13617−13633.
(63) Fuchsel, G.; Zhou, X.; Jiang, B.; Juaristi, J. I.; Alducin, M.; Guo, H.; Kroes, G.-J. Reactive and Nonreactive Scattering of HCl from Au (111): An Ab Initio Molecular Dynamics Study. *J. Phys. Chem. C* **2019**, *123*, 2287−2299.
(64) Zhang, Y.; Maurer, R. J.; Guo, H.; Jiang, B. Hot-electron effects during reactive scattering of H 2 from Ag (111): the interplay between mode-specific electronic friction and the potential energy landscape. *Chem. Sci.* **2019**, *10*, 1089−1097.

https://dx.doi.org/10.1021/acs.jpca.9b10698
J. Phys. Chem. A XXXX, XXX, XXX−XXX

(65) Dou, W.; Subotnik, J. E. Universality of electronic friction: Equivalence of von Oppen's nonequilibrium Green's function approach and the Head-Gordon−Tully model at equilibrium. *Phys. Rev. B: Condens. Matter Mater. Phys.* **2017**, *96*, 104305.
(66) Dou, W.; Subotnik, J. E. Universality of electronic friction. II. Equivalence of the quantum-classical Liouville equation approach with von Oppen's nonequilibrium Green's function methods out of equilibrium. *Phys. Rev. B: Condens. Matter Mater. Phys.* **2018**, *97*, 064303.
(67) Dou, W.; Ochoa, M. A.; Nitzan, A.; Subotnik, J. E. Universal approach to quantum thermodynamics in the strong coupling regime. *Phys. Rev. B: Condens. Matter Mater. Phys.* **2018**, *98*, 134306.
(68) Bartels, C.; Cooper, R.; Auerbach, D. J.; Wodtke, A. M. Energy transfer at metal surfaces: the need to go beyond the electronic friction picture. *Chem. Sci.* **2011**, *2*, 1647−1655.
(69) Wodtke, A. M.; Tully, J. C.; Auerbach, D. J. Electronically non-adiabatic interactions of molecules at metal surfaces: Can we trust the Born-Oppenheimer approximation for surface chemistry? *Int. Rev. Phys. Chem.* **2004**, *23*, 513.
(70) Shenvi, N.; Roy, S.; Tully, J. C. Nonadiabatic scattering at metal surfaces: independent-electron surface hopping. *J. Chem. Phys.* **2009**, *130*, 174107.
(71) Shenvi, N.; Roy, S.; Tully, J. C. Dynamical Steering and Electronic Excitation in NO Scattering from a Gold Surface. *Science* **2009**, *326*, 829−832.
(72) Miao, G.; Ouyang, W.; Subotnik, J. A comparison of surface hopping approaches for capturing metal-molecule electron transfer: A broadened classical master equation versus independent electron surface hopping. *J. Chem. Phys.* **2019**, *150*, 041711.
(73) Dou, W.; Nitzan, A.; Subotnik, J. E. Surface hopping with a manifold of electronic states. II. Application to the many-body Anderson-Holstein model. *J. Chem. Phys.* **2015**, *142*, 084110.
(74) Dou, W.; Nitzan, A.; Subotnik, J. E. Frictional effects near a metal surface. *J. Chem. Phys.* **2015**, *143*, 054103.
(75) Dou, W.; Subotnik, J. E. A broadened classical master equation approach for nonadiabatic dynamics at metal surfaces: Beyond the weak molecule-metal coupling limit. *J. Chem. Phys.* **2016**, *144*, 024116.
(76) Dou, W.; Schinabeck, C.; Thoss, M.; Subotnik, J. E. A broadened classical master equation approach for treating electron-nuclear coupling in non-equilibrium transport. *J. Chem. Phys.* **2018**, *148*, 102317.
(77) Tully, J. C. CHEMICAL DYNAMICS AT METAL SURFACES. *Annu. Rev. Phys. Chem.* **2000**, *51*, 153.
(78) Kruger, B. C.; Bartels, N.; Bartels, C.; Kandratsenka, A.; Tully, J. C.; Wodtke, A. M.; Schafer, T. NO vibrational energy transfer on a metal surface: Still a challenge to first-principles theory. *J. Phys. Chem. C* **2015**, *119*, 3268−3272.
(79) Jiang, B.; Guo, H. Dynamics in reactions on metal surfaces: A theoretical perspective. *J. Chem. Phys.* **2019**, *150*, 180901.
(80) Park, G. B.; Krüger, B. C.; Borodin, D.; Kitsopoulos, T.; Wodtke, A. M. Fundamental mechanisms for molecular energy conversion and chemical reactions at surfaces. *Rep. Prog. Phys.* **2019**, *82*, 096401.
(81) Rittmeyer, S. P.; Bukas, V. J.; Reuter, K. Energy dissipation at metal surfaces. *Advances in Physics: X* **2018**, *3*, 1381574.
(82) Jiang, B.; Yang, M.; Xie, D.; Guo, H. Quantum dynamics of polyatomic dissociative chemisorption on transition metal surfaces: mode specificity and bond selectivity. *Chem. Soc. Rev.* **2016**, *45*, 3621−3640.
(83) Anderson, P. W. Localized Magnetic States in Metals. *Phys. Rev.* **1961**, *124*, 41−53.
(84) Holstein, T. Studies of polaron motion: Part I. The molecular-crystal model. *Ann. Phys.* **1959**, *8*, 325−342.
(85) NEWNS, D. M. Self-Consistent Model of Hydrogen Chemisorption. *Phys. Rev.* **1969**, *178*, 1123−1135.
(86) Head-Gordon, M.; Tully, J. C. Vibrational relaxation on metal surfaces: Molecular-orbital theory and application to CO/Cu (100). *J. Chem. Phys.* **1992**, *96*, 3939−3949.
(87) Schäfer, T.; Bartels, N.; Golibrzuch, K.; Bartels, C.; Köckert, H.; Auerbach, D. J.; Kitsopoulos, T. N.; Wodtke, A. M. Observation of direct vibrational excitation in gas-surface collisions of CO with Au (111): a new model system for surface dynamics. *Phys. Chem. Chem. Phys.* **2013**, *15*, 1863−1867.
(88) Schmidt, J. R.; Parandekar, P. V.; Tully, J. C. Mixed quantum-classical equilibrium: Surface hopping. *J. Chem. Phys.* **2008**, *129*, 044104.
(89) Subotnik, J. E.; Ouyang, W.; Landry, B. R. Can we derive Tully's surface-hopping algorithm from the semiclassical quantum Liouville equation? Almost, but only with decoherence. *J. Chem. Phys.* **2013**, *139*, 214107.
(90) Larsen, R. E.; Bedard-Hearn, M. J.; Schwartz, B. J. Exploring the Role of Decoherence in Condensed-Phase Nonadiabatic Dynamics: A Comparison of Different Mixed Quantum/Classical Simulation Algorithms for the Excited Hydrated Electron. *J. Phys. Chem. B* **2006**, *110*, 20055.
(91) Jain, A.; Alguire, E.; Subotnik, J. E. An Efficient, Augmented Surface Hopping Algorithm That Includes Decoherence for Use in Large-Scale Simulations. *J. Chem. Theory Comput.* **2016**, *12*, 5256.
(92) Dou, W.; Subotnik, J. E. A generalized surface hopping algorithm to model non-adiabatic dynamics near metal surfaces: The case of multiple electronic orbitals. *J. Chem. Theory Comput.* **2017**, *13*, 2430−2439.
(93) Dou, W.; Nitzan, A.; Subotnik, J. E. Molecular electronic states near metal surfaces at equilibrium using potential of mean force and numerical renormalization group methods: Hysteresis revisited. *J. Chem. Phys.* **2016**, *144*, 074109.
(94) Kapral, R. Progress in the theory of mixed quantum-classical dynamics. *Annu. Rev. Phys. Chem.* **2006**, *57*, 129−157.
(95) Shi, Q.; Geva, E. A derivation of the mixed quantum-classical Liouville equation from the influence functional formalism. *J. Chem. Phys.* **2004**, *121*, 3393.
(96) Lü, J.-T.; Hu, B.-Z.; Hedegård, P.; Brandbyge, M. Semi-classical generalized Langevin equation for equilibrium and nonequilibrium molecular dynamics simulation. *Prog. Surf. Sci.* **2019**, *94*, 21.
(97) Nitzan, A. *Chemical dynamics in condensed phases: relaxation, transfer and reactions in condensed molecular systems*; Oxford University Press, 2006.
(98) Ouyang, W.; Dou, W.; Jain, A.; Subotnik, J. E. Dynamics of Barrier Crossings for the Generalized Anderson−Holstein Model: Beyond Electronic Friction and Conventional Surface Hopping. *J. Chem. Theory Comput.* **2016**, *12*, 4178−4183.
(99) Interestingly, note that the shape of BCME as a function of Γ resembles the electron transfer rate in solution, i.e., without a metal; see Figure 1 in ref 134.
(100) Gosavi, S.; Marcus, R. Nonadiabatic electron transfer at metal surfaces. *J. Phys. Chem. B* **2000**, *104*, 2067−2072.
(101) Nitzan, A. Electron transmission through molecules and molecular interfaces. *Annu. Rev. Phys. Chem.* **2001**, *52*, 681−750.
(102) Coffman, A. J.; Subotnik, J. E. When is electronic friction reliable for dynamics at a molecule−metal interface? *Phys. Chem. Chem. Phys.* **2018**, *20*, 9847−9854.
(103) Kaasbjerg, K.; Novotný, T.; Nitzan, A. Charge-carrier-induced frequency renormalization, damping, and heating of vibrational modes in nanoscale junctions. *Phys. Rev. B: Condens. Matter Mater. Phys.* **2013**, *88*, 201405.
(104) Siddiqui, L.; Ghosh, A. W.; Datta, S. Phonon runaway in carbon nanotube quantum dots. *Phys. Rev. B: Condens. Matter Mater. Phys.* **2007**, *76*, 085433.
(105) Koch, J.; Semmelhack, M.; von Oppen, F.; Nitzan, A. *Phys. Rev. B: Condens. Matter Mater. Phys.* **2006**, *73*, 155306.
(106) Shenvi, N.; Tully, J. C. Nonadiabatic dynamics at metal surfaces: Independent electron surface hopping with phonon and electron thermostats. *Faraday Discuss.* **2012**, *157*, 325−335.
(107) Dou, W.; Subotnik, J. E. A many-body states picture of electronic friction: The case of multiple orbitals and multiple electronic states. *J. Chem. Phys.* **2016**, *145*, 054102.
(108) Landry, B. R.; Falk, M. J.; Subotnik, J. E. Communication: The correct interpretation of surface hopping trajectories: How to calculate electronic properties. *J. Chem. Phys.* **2013**, *139*, 211101.

https://dx.doi.org/10.1021/acs.jpca.9b10698
J. Phys. Chem. A XXXX, XXX, XXX−XXX

(109) Kapral, R. Surface hopping from the perspective of quantum−classical Liouville dynamics. *Chem. Phys.* **2016**, *481*, 77−83.
(110) Subotnik, J. E.; Jain, A.; Landry, B.; Petit, A.; Ouyang, W.; Bellonzi, N. Understanding the Surface Hopping View of Electronic Transitions and Decoherence. *Annu. Rev. Phys. Chem.* **2016**, *67*, 387.
(111) Volobuev, Y. L.; Hack, M. D.; Topaler, M. S.; Truhlar, D. G. Continuous surface switching: An improved time-dependent self-consistent-field method for nonadiabatic dynamics. *J. Chem. Phys.* **2000**, *112*, 9716.
(112) Hack, M. D.; Truhlar, D. G. Electronically nonadiabatic trajectories: Continuous surface switching II. *J. Chem. Phys.* **2001**, *114*, 2894−2902.
(113) Jasper, A. W.; Hack, M. D.; Truhlar, D. G. The treatment of classically forbidden electronic transitions in semiclassical trajectory surface hopping calculations. *J. Chem. Phys.* **2001**, *115*, 1804−1816.
(114) Zhu, C.; Jasper, A. W.; Truhlar, D. G. Non-Born−Oppenheimer trajectories with self-consistent decay of mixing. *J. Chem. Phys.* **2004**, *120*, 5543−5557.
(115) Webster, F.; Rossky, P. J.; Friesner, R. Nonadiabatic processes in condensed matter: semi-classical theory and implementation. *Comput. Phys. Commun.* **1991**, *63*, 494−522.
(116) Wong, K. F.; Rossky, P. J. Dissipative mixed quantum-classical simulation of the aqueous solvated electron system. *J. Chem. Phys.* **2002**, *116*, 8418−8428.
(117) Schwartz, B. J.; Bittner, E. R.; Prezhdo, O. V.; Rossky, P. J. Quantum decoherence and the isotope effect in condensed phase nonadiabatic molecular dynamics simulations. *J. Chem. Phys.* **1996**, *104*, 5942−5955.
(118) Subotnik, J. E.; Shenvi, N. A new approach to decoherence and momentum rescaling in the surface hopping algorithm. *J. Chem. Phys.* **2011**, *134*, 024105.
(119) Shenvi, N.; Subotnik, J. E.; Yang, W. Simultaneous-trajectory surface hopping: A parameter-free algorithm for implementing decoherence in nonadiabatic dynamics. *J. Chem. Phys.* **2011**, *134*, 144102.
(120) Tao, X.; Shushkov, P.; Miller, T. F., III Path-integral isomorphic Hamiltonian for including nuclear quantum effects in non-adiabatic dynamics. *J. Chem. Phys.* **2018**, *148*, 102327.
(121) Shakib, F. A.; Huo, P. Ring Polymer Surface Hopping: Incorporating Nuclear Quantum Effects into Nonadiabatic Molecular Dynamics Simulations. *J. Phys. Chem. Lett.* **2017**, *8*, 3073−3080.
(122) Hele, T. J. Thermal quantum time-correlation functions from classical-like dynamics. *Mol. Phys.* **2017**, *115*, 1435−1462.
(123) Lawrence, J. E.; Manolopoulos, D. E. Analytic continuation of Wolynes theory into the Marcus inverted regime. *J. Chem. Phys.* **2018**, *148*, 102313.
(124) Jang, S.; Voth, G. A. A derivation of centroid molecular dynamics and other approximate time evolution methods for path integral centroid variables. *J. Chem. Phys.* **1999**, *111*, 2371−2384.
(125) Markland, T. E.; Ceriotti, M. Nuclear quantum effects enter the mainstream. *Nat. Rev. Chem.* **2018**, *2*, 0109.
(126) Ceperley, D. M. Path integrals in the theory of condensed helium. *Rev. Mod. Phys.* **1995**, *67*, 279−355.
(127) Liu, X.; Liu, J. Path integral molecular dynamics for exact quantum statistics of multi-electronic-state systems. *J. Chem. Phys.* **2018**, *148*, 102319.
(128) Robertson, C.; Habershon, S. Harmonic-phase path-integral approximation of thermal quantum correlation functions. *J. Chem. Phys.* **2018**, *148*, 102316.
(129) Cendagorta, J. R.; Bačić, Z.; Tuckerman, M. E. An open-chain imaginary-time path-integral sampling approach to the calculation of approximate symmetrized quantum time correlation functions. *J. Chem. Phys.* **2018**, *148*, 102340.
(130) Ananth, N.; Miller, T. F., III Exact quantum statistics for electronically nonadiabatic systems using continuous path variables. *J. Chem. Phys.* **2010**, *133*, 234103.
(131) Liu, Z.-F.; Egger, D. A.; Refaely-Abramson, S.; Kronik, L.; Neaton, J. B. Energy level alignment at molecule-metal interfaces from an optimally tuned range-separated hybrid functional. *J. Chem. Phys.* **2017**, *146*, 092326.
(132) Jorn, R.; Seideman, T. Implications and applications of current-induced dynamics in molecular junctions. *Acc. Chem. Res.* **2010**, *43*, 1186−1194.
(133) Joachim, C.; Ratner, M. A. Molecular electronics: Some views on transport junctions and beyond. *Proc. Natl. Acad. Sci. U. S. A.* **2005**, *102*, 8801.
(134) Huo, P.; Miller, T. F.; Coker, D. F. Communication: Predictive partial linearized path integral simulation of condensed phase electron transfer dynamics. *J. Chem. Phys.* **2013**, *139*, 151103.

https://dx.doi.org/10.1021/acs.jpca.9b10698
J. Phys. Chem. A XXXX, XXX, XXX−XXX